MAGISTERARBEIT

Titel der Magisterarbeit

Spectroscopic and Photometric Analysis of Pre-Main Sequence Stars in Young Open Clusters

Verfasser

Mag.^{a} Susanne Pollack-Drs, Bakk.

angestrebter akademischer Grad

Magistra der Naturwissenschaften (Mag.rer.nat.)

Wien, April 2012

Studienkennzahl:	A 066 861
Studienrichtung	Magisterstudium Astronomie
Betreuerin:	Dr. Konstanze Zwintz

Abstract

The content of the first part of this work includes the search and identification of pulsating pre-main sequence stars in the young open cluster NGC 6611. The measurements were obtained during 10 out of 14 nights with the 0.9 m telescope of the Cerro Tololo Interamerican Observatory (CTIO) in Chile. The analysis was based on continuous time series of CCD photometry, using Johnson B & V filters. The detailed frequency analysis was carried out using the `Period04` software (Lenz et al., 2005). A second run of frequency analyses was performed additionally with the program `SigSpec` (SIGnificance SPECtrum, Reegen 2004 and 2007), to confirm the frequencies identified with `Period04`. In total 4 out of the 186 selected stars showed significant pulsating frequencies. The remaining 182 stars were either inconclusive or constant and need further investigation.

In the second part of this study a selection of previously identified pulsating pre-main sequence stars of the three young open clusters NGC 6611, NGC 6530 and NGC 6383 were analyzed spectroscopically to derive fundamental parameters, i. e. effective temperature, surface gravity and $v \cdot \sin i$ values. Previously, only for a few stars spectral classes were available in the literature. All classification spectra were observed with the R-C spectrograph at the CTIO 1.5 m telescope in the wavelength range from 4050 Å to 4700 Å. This wavelength range includes the typical lines for the classification of A and F type stars, i. e. hydrogen Balmer lines, Ca II, Fe I and Mg II. Each spectrum was compared with Kurucz models. Several stars showed lines in emission.

Zusammenfassung

Der erste Teil der Arbeit widmet sich der Suche und Identifizierung von pulsierenden Vorhauptreihensternen im jungen Sternhaufen NGC 6611. Der Sternhaufen wurde am Cerro Tololo Interamerican Observatory (CTIO) in Chile 10 Nächte lang beobachtet. Aufgenommen wurde eine Zeitserien-Photometrie in den beiden Johnson Filtern B und V. Die Daten wurden mithilfe des Programms `Period04` (Lenz et al., 2005) analysiert. Zusätzlich wurden die Frequenzen mit dem Program `SigSpec` (SIGnificance SPECtrum, Reegen 2004 and 2007) bestimmt. Von den 186 ausgewählten Sternen zeigten vier Sterne eine deutlich signifikante Pulsation. Die verbliebenen 182 Sterne erwiesen sich als konstant oder nicht eindeutig als pulsierend klassifizierbar.

Im zweiten Teil dieser Arbeit werden bereits zuvor klassifizierte pulsierende Vorhauptreihensterne aus den drei jungen Sternhaufen NGC 6611, NGC 6383 und NGC 6530 spektroskopisch untersucht. Da zuvor sehr wenig über die untersuchten Sterne in der Literatur bekannt war, ist das Ziel dieser Analyse die Bestimmung der Fundamentalparameter, wie zum Beispiel die Effektivtemperatur, log g und $v \cdot \sin i$. Alle Klassifikationsspektren wurden mit dem R-C Spektrographen am CTIO 1.5 m Teleskop im Wellenlängenbereich von 4050 Å bis 4700 Å aufgenommen. In diesen Wellenlängenbereich fallen die für A und F Sterne charakteristischen Linien, wie zum Beispiel, die H-Linien der Balmerserie, sowie Ca II, Fe I und Mg II. Jedes Spektrum wurde mit Kurucz Modellen verglichen und ausgewertet. Einige der untersuchten Sterne enthielten Emissionslinien in ihren Spektren.

Contents

Chapter 1

Pre-main sequence stellar evolution

1.1 Early stellar evolution

The investigation of stellar evolution is a very active research field. One of the most fundamental questions is to understand the formation of stars which condense out of a molecular cloud (de Winter et al., 1991). Star formation is still an ongoing process and happens all over the universe. The molecular cloud starts to collapse, when gravitational forces exceed the outward pressure forces. Rotational processes flatten the interstellar cloud and an accretion disk evolves. In the center of this disk a protostar is formed, which is not in a hydrostatic equilibrium. The hydrostatic equilibrium is reached, when the outward pressure forces and the gravitation forces are balanced. On the so-called Hayashi track the young star becomes mainly hydrostatic for the first time (Weigert et al., 2005). From this Hayashi track stars are contracting towards the zero-age main sequence (ZAMS) depending on their masses. On the ZAMS the radiated energy from the photosphere is equal to the nuclear energy production in the interior. The first visible appearance of stars in the Hertzsprung-Russell (HR-) diagram is the so called birthline (Stahler 1983). The phase between the contraction of the stars from the birthline to the ZAMS is called the pre-main sequence phase. This evolutionary stage lasts till the hydrogen burning starts and the star becomes a main sequence star.

1.1.1 Pre-main sequence stars

High mass stars, O and early B-type stars, with masses higher than 10 $M_{\odot}$, do not have an optically visible pre-main sequence phase. They reach the main sequence still surrounded by their protostellar envelope, appearing as a H II region, and can only be observed in the IR as accreting protostars or in their later evolutionary stages. Low-mass stars of spectral type F to G lose their envelope on the Hayashi track and get optically visible with their protostellar disks.These highly active stars are named T Tauri stars. The envelopes of intermediate mass stars of spectral types B to A, become transparent on their way towards the main sequence. Stars of this group are named as Herbig-Ae/Be stars (Weigert et al., 2005).

Pre-main sequence stars in general are strongly interacting with the circumstellar matter in which they are still embedded (Stahler et al., 2006). They are characterized by an intense surface activity that includes winds, accretion, fast rotation, X-ray emissions and variable obscuration from circumstellar dust (Marconi et al., 2004) . Another major property of pre-main sequence stars is the high infrared excess in their spectral energy distributions due to circumstellar dust, often accompanied by strong emission lines (de Winter et al., 1991). The more or less strong IR-excess is caused by a disk or cocoon around the central star (Martayan et al., 2007). Spectroscopic and photometric variabilities are observed in pre-main sequence stars on time scales from minutes to years, indicating that stellar activity begins in the earliest phases of stellar evolution, prior to the arrival on the main sequence (Zwintz 2005). On their way towards the main sequence young stars pass the so called instability strip. Some pre-main sequence stars show pulsations in or near this region. These pulsations result in luminosity variations on time scales of half an hour to some hours due to physical changes within the star. With asteroseismology it is possible to get more information about the internal structure of a star.

The theory of stellar evolution adresses stars that are in hydrostatic equilibrium. To determine the initial conditions of stellar evolution, like masses, radii and internal structure, at the moment when young stars become mainly hydrostatic for the first time, is the main problem to be solved. Another unanswered question are the initial conditions of stars at the beginning of their pre-main sequence evolutionary tracks in the Hertzsprung-Russell diagram. The study of pre-main sequence stars should help to possibly answer those questions in the future.

As mentioned above pre-main sequence stars can be divided into two groups depending on their masses: T Tauri stars and Herbig Ae/Be stars.

1.1.2 T Tauri stars

T Tauri stars are young low mass stars, with masses lower than 2 $M_{\odot}$, that have recently become visible in the optical range at the Hayashi track. They were first discovered by Joy in 1942 within the Taurus-Auriga dark cloud. T Tauri stars are very active with a spectral range from F to M and are associated with high nebulosity. According to Herbig (1963) the spectra of T Tauri stars show a lot of lines in emission, like H, Ca II, K and Fe I. Fluorescent Fe I emission lines at λ = 4063 Å and λ = 4132 Å are also present, which only have been found in T Tauri stars (Bastian et al. 1983). Sometimes there are also SII emission lines visible at λ = 4068 Å and λ = 4076 Å (Bastian et al., 1983). Also the presence of the strong absorption line of Li I at λ = 6707 Å is taken as a criterion for T Tauri stars. Features like the strong Hα, the far-IR emission and the forbidden lines in some stars cannot be explained yet. These indicate the presence of gas and dust in a more extended region around the stars. T Tauri stars are variable with a variability ranging from minutes to years and at different wavelengths. Because T Tauri stars are of later spectral type and are not lying within the instability region of the HR-diagram, they are not the prime candidates to study pulsations.

1.1.3 Herbig Ae/Be stars

Herbig Ae/Be stars - first detected by Herbig (1959) - possess higher masses and higher effective temperatures than T Tauri stars (Talavera 1998). Their masses range between 2 and 10 $M_{\odot}$. The lower limit is corresponding to the mass above which stars are radiatively stable when they begin their quasistatic contraction. The upper limit corresponds to the mass above which stars start with the hydrogen burning before they emerge from their contracting envelope (Stahler 1983). According to Vieira et al. (2003) Herbig Ae/Be stars have the following characteristics:

- They have spectral types of A or B.
- Emission lines are present within their spectra, e.g. Balmer lines, Ca II, Fe I.
- The stars are located in an obscured region associated with a bright nebulosity in its vicinity.
- They illuminate reflection nebulae in their vicinity.
- The stars possess an infrared excess due to hot or cool cirumstellar dust or both.
- They are photometrically variable.

Herbig Ae/Be stars display regular and irregular light variations on different time scales. For example, photometric variabilities on time scales of weeks are a result of variable extinction due to circumstellar dust. Also variabilities on time scales longer than a day have been studied frequently. If the star is crossing the region of the instability strip in the HR-diagram and the variability shows a period between half an hour and few hours, the origin of the variability is pulsation (Zwintz 2005).

Herbig Ae/Be stars are also known to be variable in their spectral lines. There is a variability for example in their Hα line profiles (e.g. Catala 1994, Reipurth et al., 1996, Vieira et al., 2003). The Hα line profiles can be divided into four groups: a) symmetric profiles with only shallow absorption features, b) double-peaked line profiles, with the second peak having more strength than the first one, c) double-peaked line profiles with the first one bigger than the second and d) line profiles with P Cyg line characteristics (Vieira et al., 2003). These stellar features are possible indicators for Herbig Ae/Be stars having an accreting circumstellar disk (Carmona et al., 2010) and are remarkable signs of activity and winds (Boehm et al., 1995). There are several other debates about the origin of the double lined profiles, like magnetic fields and rotation (Reipurth et al., 1996) in the literature.

The existing infrared excess is interpreted as an emission from small dust grains present in the hot surface layer of the disk (Carmona et al., 2010). Analysing the nature of such disks is important for the understanding of stellar evolution and moreover such disks are the sites of planet formation (Carmona et al. 2010). All their properties together make these stars ideal candidates to search for pulsating pre-main sequence stars, because pre-main sequence stars with masses between 1.5 and 4 $M_{\odot}$ have the ideal combination of temperature, luminosity and mass to become vibrationally unstable (Zwintz et al., 2006).

1.1.4 Pulsating pre-main sequence stars

The detection of pulsation in pre-main sequence stars is of great importance for understanding the internal structure of young stars. The first evidence for the existence of pulsating pre-main sequence stars was adduced by Breger (1972) in the young open cluster NGC 2264. He discovered two δ Scuti-like pulsators, V 588 Mon (HD 261331) and V 589 Mon (HD 261446). More than 20 years passed before the detection of the next pulsating pre-main sequence star HR 5999 (HD 144668) happened by Kurtz & Marang (1995).

Stellar oscillations offer the opportunity to gather information about the internal structure and processes of a star. The different modes penetrate to different depths in the star and deliver the information from the interior.

There are two kinds of oscillation modes: p-modes (pressure modes) and g modes (gravity modes). For the p modes pressure is the restoring force. The p modes are acoustic waves and have gas motions that are primarily vertical. For the gravity modes the restoring force of the pulsation is buoyancy and the gas motions are primarily horizontal (Aerts et al., 2010). The p modes are very sensitive to conditions in the outer part of a star, whereas g modes are most sensitive to those of the deep interior. Since p-modes are acoustic waves for modes that are not directed at the center of the star, the lower part of the wave is in a higher temperature environment than the upper part, that means in a region of higher sound speed. The consequence is that the wave is refracted back to the surface, where it is then reflected. High degree modes penetrate only to a shallow depth, whereas lower degree modes penetrate more deeply. The frequency of the mode observed on the surface depends on the sound travel time along its path. The aim is to get enough frequencies over the different ranges to built a map of the interior sound speed, to deduce temperature, pressure, density, chemical composition and rotation (Aerts et al., 2010).

The simplest modes are the radial modes where the star swells and contracts, heat and cools, spherically symmetrically with the core as a node and the surface as a displacement antinode. The simplest nonradial mode is the axisymmetric dipole mode, for which the equator is a node. That means that the northern hemisphere swells up while the southern hemisphere contracts and vice versa. One hemisphere cools and the other heats (Aerts et al., 2010).

The driving mechanisms of pulsations can be on the one hand heat-engine mechanisms or on the other hand they are connected with opacity, known as the κ mechanism. For high opacity hydrogen and helium is needed to make the κ mechanism work. In the ionization layers containing hydrogen and helium opacity blocks radiation, the gas heats and the increasing pressure causes a swelling of the star past its equilibrium point. Because of the reduction of the opacity by the ionization, radiation flows through and the gas is allowed to cool. The weight of the overlying layers can no longer be supported by the gas and the star contracts. On contraction the hydrogen and helium recombines, the flux gets absorbed and the layer gets heat on compression again (Aerts et al., 2010). One part of the radiation energy is transformed into oscillation energy. The pre-main sequence stars contract towards the main sequence, either radiatively like the Herbig Ae/Be stars or convectively like the T Tauri stars (Aerts et al., 2010). The high variability of these stars results on the one hand from their interactions with the circumstellar environment and on the other hand the shorter period variabilities are due to oscillations. The oscillation spectra enables the distinction between the two evolutionary stages for stars with the same effective temperature and luminosity, because the interior structure of PMS-stars is different from that of evolved stars. Within pre-main sequence stars two kinds of pulsations can be expected: δ Scuti- and γ Doradus-like pulsations.

δ Scuti like stars are of the spectral range A to F, lie near or above the main sequence and pulsate with periods between 18 minutes and 6.5 hours. The energy source for the pulsation is driven by the κ mechanism in the He II ionization zone near 48 000 K (Zwintz, 2005). Within δ Scuti stars radial and nonradial oscillations occur. Those are generally low order p modes. The amplitudes range from mmag up to tenths of a magnitude (Aerts et al., 2010). In some cases also mixed modes can occur. That means that there is for example a g-mode character in the interior and a p-mode character in the outer layers of a star. Those kind of oscillations only might appear in more evolved stars, which have already evolved off the main sequence and are undergoing hydrogen shell burning (Aerts et al., 2010).

γ Doradus like stars have early-F spectral types and show a mulitperiodic behaviour with individual periods between 0.5 and 3 days. Their variability is interpreted in terms of mulitperiodic high order nonradial g modes (Aerts et al., 2010). They possess a convective core, a radiative envelope and a smaller outer convective zone close to the photosphere (Kaye et al., 1999). The actually presented driving mechanism for the γ Doradus like pulsation is similar to convective blocking in the relatively thin convective envelopes of these stars (Guzik et al., 2000). The γ Doradus stars are very challenging objects, because of the long periods and the fact that they can undergo at the same time g-modes and solar-like p-modes (Aerts et al., 2010).

In the mean time there are 64 known or suspected pre-main sequence candidates for pulsation. It is important to increase the number of pulsating pre-main sequence stars to be able to define the PMS instability strip observationally (Zwintz 2005) and to test the correctness of the existing models, because the accurate effective temperatures and luminosities, with which the models are constrained, are often not available for young stars (Guenther et al., 2007). Furthermore for pulsating pre-main sequence stars located within a cluster, the cluster membership can be confirmed and an independent estimation of the age and distance for the cluster can be performed under the aid of asteroseismology.

Chapter 2

NGC 6611, NGC 6383 and NGC 6530

2.1 NGC 6611

NGC 6611 ($\alpha_{2000} = 18^{h}\,18^{m}.7$, δ_{2000} = -13° 47.1') is a young cluster located in the constellation of Serpens embedded in the Sagittarius spiral arm and is associated with the emission nebula M 16, the Eagle Nebula (de Winter et al., 1997). Belikov et al. (1999) classified the distance of the cluster with 2.14 ± 0.10 kpc which was confirmed by Th$\acute{e}$ et al. (1990). A high and variable reddening, leading to an anomalous extinction law, was measured by different authors (Hillenbrand et al., 1993; de Winter et al., 1997). This was also confirmed by Chini & Neckel (1981). According to Sagar and Joshi (1979) the cluster reddening varies between an E(B-V) = $0^{m}.58$ and an E(B-V) =$1^{m}.21$, and the extinction is larger in the northern part of the cluster than it is in the southern.

NGC 6611 is a very young cluster and therefore an ideal research field to study star formation and evolution. It is obscured by dark dense clouds and a lot of dust, that make the observations of its stellar content quite difficult. The cluster stars are not of a uniform age. There is an age-spread from 0.25 Myr up to 2 Myr (Hillenbrand et al. 1993). Hillenbrand et al. (1993) derived a star population of high mass stars which belong to the older age and a large group of intermediate-mass stars (3-8 $M_{\odot}$) belonging to the younger. Using infrared imaging additionally to CCD photometry and spectroscopy Hillenbrand et al. (1993) investigated the existence of circumstellar disks. They differed between main-sequence and pre-main-sequence stars. So the long expected occurrence of pre-main sequence stars was confirmed. Hillenbrand et al. (1993) also detected a not significant amount of emission line stars.

Figure 2.1: This figure shows a DSS image of NGC 6611

Based on these results de Winter et al. (1997) focussed their observations on the stellar content of NGC 6611 with special attention to pre-main sequence stars. They observed 49 stars and divided the stellar content into three groups. Their group I includes stars which fit to the main-sequence and are entering the post-main-sequence stadium, including very luminous stars with a strong infrared excess. The second group II includes stars which are obviously surrounded by dust and are pre-main-sequence stars. Group III covers those stars which have no abnormal extinction, are luminous and of a late spectral type. De Winter et al. (1997) classified them to be foreground objects. Furthermore they tried to derive membership probabilities based on E(B-V) values. According to de Winter et al. (1997) a star is a cluster member, when its E(B-V) value is larger than $0^{\mathrm{m}}.50$.

Tucholke et al. (1986) focused their investigations on the membership probabilities from proper motion studies. They concentrated in their studies especially on pre-main sequence stars classified by Walker (1961). Over the years these pre-main sequence stars had been subject of a lot of discussions. Most of these stars were classified as foreground objects, but Tucholke et al. (1986) could prove that ten stars out of them are really pre-main sequence stars. Chini & Wargau (1990) took the reddening law and the extinction into account to distinguish between cluster members and foreground stars. Furthermore they wanted to address the question which stars are really pre-main sequence objects and which are foreground stars. Only stars which have a $(B - V)_0$ larger than 0.15 mag and a V_0 larger than 2 mag were treated as pre-main sequence stars.

Guarcello et al. (2007 and 2009) analysed the stellar content for the existence of circumstellar disks, Bosch et al. (1999) for binaries and Martayan et al. (2008) investigated the Be-phenomenon (i.e. a period of spectral emissions caused by the presence of a circumstellar envelope around a Be star).

In this work on the one hand the focus lies on the detection of pulsating pre-main-sequence stars and on the other on deriving fundamental parameters like effective temperature, surface gravity and $v \cdot \sin i$ of selected pre-main sequence stars.

2.2 NGC 6530

Another young cluster is NGC 6530 ($\alpha_{2000} = 18^{\mathrm{h}}\ 04^{\mathrm{m}}.5$, δ_{2000} = -24° 22'). It is associated with the emission nebula and H II region M8, the Lagoon nebula. The cluster age was estimated to be about 2 Myr by van Altena & Jones (1972). Its distance is about 1780 pc (van Altena et al., 1972) and the colour excess E(B - V) = 0.39 mag (Chini et al., 1981).

One of the first studies performed on this cluster were carried out by Walker (1957). Two luminous O type stars HD 164794 and HD 165052 were detected on opposite sides of the cluster. Walker (1957) also proposed an anomalous reddening of the cluster and the presence of pre-main-sequence stars. The colour-magnitude diagram of NGC 6530 contains stars from spectral type O 5 to A 0 and later, lying on the main sequence (Chini et al., 1981). Proper motion studies performed by van Altena & Jones (1972) helped to determine the stellar content distinguishing between field stars and probable cluster members. Most of Walker's pre-main sequence stars turned out to be probable field stars. Investigations of Hiltner et al. (1965) classified a large number of Be stars with emission lines and stars from the inner part of the cluster showing strong Hγ lines. They were not sure, if the emission lines were a result of the surrounding emission nebula or intrinsic. A multiwavelength study performed by van den Ancker et al. (1997) detected 11 suspected variable stars, nine stars showing an infrared excess and five stars with Hα emission lines out of 132 probable cluster members. Van den Ancker et al. (1997) also classified three Herbig Ae/Be stars. Furthermore van den

Figure 2.2: This figure shows a DSS image of NGC 6530.

Ancker et al. (1997) found evidence for the existence of an obscuring dark cloud within the cluster region. Due to this, every star has its own extinction law.

This star cluster too, seems to be an ideal research field for pulsating pre-main-sequence stars. A study performed by Zwintz et al. (2006) regarding pulsating pre-main sequence stars, discovered six new pre-main sequence pulsators and one suspected variable star. For most of them no spectral types are available in the literature. Therefore a spectral classification is performed for these stars to derive the fundamental parameters.

2.3 NGC 6383

NGC 6383 (α_{2000} = 17^{h} $34^{m}.8$, δ_{2000} = -32° 34‘) is a young open cluster, which is not embedded in a star forming region (Thé et al., 1985). A bright spectroscopic binary HD 159176, an O type star, is located in the central part of the cluster and induces a weak nebula S11 (Sharpless 1953). Eggen (1961) compared the HR diagram of NGC 6383 to that of NGC 2264 and concluded that NGC 6383 must be of a young age. The ages spread from 1.7 ± 0.4 Myr (FitzGerald et al., 1978) up to 4-5 Myr (Lloyd Evans, 1978). NGC 6383 belongs to the Sgr OB1 association together with NGC 6611 and NGC 6530, the other two clusters addressed in this work.

Figure 2.3: This figure shows a DSS image of NGC 6383.

Photometric and spectroscopic observations of this cluster were performed by different authors. Numerous studies were focused on the stellar content of the central part, because the membership probability of these stars to the cluster is the highest (FitzGerald et al., 1978). In 1961 Eggen asserted, that stars later than spectral type A0 are lying before the ZAMS. Among those stars, Thé et al. (1985) found three stars with an infrared excess, indicating the pre-main sequence nature of these stars. This infrared excess was also confirmed by van den Ancker et al. (2000) and Lloyd Evans et al. (1978). Additionally FitzGerald et al. (1978) performed spectral classifications of their stars. One of the observed stars even showed a Hα emission line.

FitzGerald et al. (1978) performed photoelectric observations and estimated the cluster reddening with E(B-V) = 0.33 ± 0.02 mag and Lloyd Evans et al. (1978) derived the reddening with E(B-V) = 0.35 ± 0.02 mag.

The age of the central binary star HD 159176 is estimated with 2.8 ± 0.5 Myr by FitzGerald et al. (1978) and therefore it is definitely older than the remaining part of the cluster core. This central star seems to generate star formation and induces the H II region. Rauw et al. (2003) performed XMM-Newton observations of NGC 6383, because pre-main sequence stars are also known X-ray sources. With their analyses they confirmed the interaction with the pre-main sequence stars and the bright central star.

Summing up all those studies, NGC 6383 is an ideal research field to investigate the nature of pre-main-sequence stars. The initial speculations about the existence of pre-main sequence stars were confirmed. Furthermore this cluster is an ideal candidate to search for pulsating pre-main-sequence stars. Zwintz et al. (2005) detected 2 new pre-main sequence pulsators within NGC 6383 and one suspected pulsator. Both stars, W 55 and W 54, and a third one, W 262, that remained inconclusive in their analyses, were subject of the spectral classification within this work.

Chapter 3

CCD Time Series Photometry of stars in NGC 6611

The light we get from stars provides us with a lot of information, which can be extracted using the two major observing techniques: photometry and spectroscopy. Over the years a lot of observing methods were developed to investigate the different properties of a star. Photometrically a star can be observed in different wavelength ranges, such as in the UV, IR and in the optical range using special filter systems. In the optical range the Johnson-UBV filter system is very common to measure the apparent magnitude of stars and is used in the present work. This system is based on three colors; where the center of gravities are at 3700 Å (ultraviolet), at 4400 Å (blue) and at 5500 Å (visual). The system is chosen in that kind, that a star of spectral type A0 has the same apparent magnitude in the ultraviolet, the visual and in the blue. The differences between the filters, like (B-V) and (U-B) build the color indices. The color index marks the temperature of the surface of a star. The larger the color index is, the redder is the star. Very often the results are shown within an CMD (color-magnitude diagram), where the color index is presented versus the apparent magnitude. Another important diagram is the HRD (Hertzsprung Russell Diagram) in which the relation between the luminosity, e.g. via an absolute magnitude, and the effective temperature, e.g. via a dereddened color index, is presented.

Open clusters include stars of about the same age and the same distance. Especially for the observation of young stars, open clusters younger than 10 Myr are the main target, because these are the locations where new stars are born. Young clusters, like NGC 6611, NGC 6383 and NGC 6530 are ideal research fields for investigating star formation and evolution. In this work photometric analyses were used to distinguish between constant and pulsating variable (pre)-main sequence stars. Asteroseismology in addition might help to understand better the internal structure of young stars. The two clusters NGC 6383 and NGC 6530 have already been subject of an earlier investigation for pulsating pre-main sequence stars (Zwintz 2005). Using CCD photometry and analyzing light curves with Fourier techniques on stars within the cluster NGC 6611 should analyze any periodic behavior and discover new pre-main sequence pulsators. Maybe the total number of already discovered pre-main sequence pulsators can be increased.

3.1 Observations

The search and identification of pulsating pre-main sequence stars (PMS) was based on continuous time series of CCD frames, using Johnson B & V filters. The measurements were obtained during 10 out of 14 nights from September 2^{nd} to September 15^{th}, 2004 with the 0.9 m telescope of the Cerro Tololo Interamerican Observatory (CTIO) in Chile. The telescope with its field of view of 13.5 x 13.5 arcminutes together with Johnson B & V filters and the dedicated 2048 x 2048 CCD detector allows to observe cluster members down to V=16 mag with the required high time resolution and low noise level. Furthermore the observing dates were close to new moon for a low sky background.

3.2 Data reduction and Frequency Analyses

3.2.1 CCD data reduction

All images were stored in the FITS-format (**F**lexible **I**mage **T**ransfer **S**ystem). Every night bias, flat-field and object frames were obtained, the latter two in both filters. An overview is given in the observing log (Table 6.1) in the APPENDIX.

Data reduction was carried out with `IRAF` [1]. The CCD chip was read out in "quad mode" by four amplifiers. Therefore the first basic reduction steps were performed using the `IRAF` `ared.quad` package. This package includes a special version of `ccdproc`, which processes multi-amplifier CCD-images. It is especially developed for the reduction of CCDs used at the CTIO observatory (Massey 1997). For the bias level subtraction, all the images were first examined with the `IRAF` task `imexamine`. The mean bias level of every quad-

[1] IRAF (http://iraf.noao.edu) distributed by the National Optical Astronomy Observatory, and operated by the Association of Universities for Research in Astronomy (AURA) under cooperative agreement with the National Science Foundation.

rant was measured and compared to the bias levels of the quadrants within the other nights. Due to small variations of these levels from night to night between the four quadrants, a master bias frame had to be created for every night using the package `quadproc` with the task `zerocombine`, which performs the combination of individual bias frames. Afterwards the masterbias was subtracted from all data frames.

The next steps consisted in combining the flat-field exposures, separately for each filter. A flat-field is the response of a detector to a uniform source of radiation. The sensitivity of each pixel in the camera is different, due to the structural variations in the CCD, caused by the filters, by dust on the CCD and by dead pixels. These pixel to pixel variations are measured by the flat-fields. Therefore a uniform source of radiation, like a dome screen, which is illuminated, for example by a tungsten lamp, is needed to receive a uniform illumination level on the CCD. A combined flat-field exposure was created separately for the B and the V filter using `flatcombine`. With the package `quadproc` all the images could be divided by the corresponding combined masterflat. Figure 3.1 shows an example for one of those created masterflats.

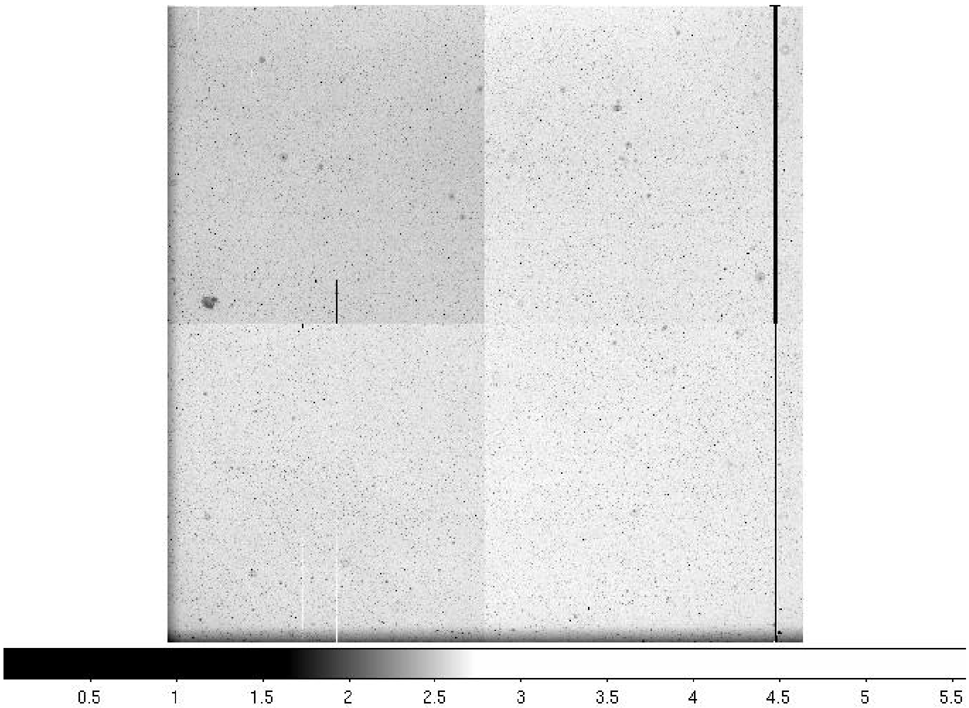

Figure 3.1: Example for a masterflat image; on the right edge a bad column is visible

As the exposure times were short (i. e. less than 100 sec), a correction for dark current was omitted. Figure 3.2 shows an example of one of the reduced object frames obtained in the B filter.

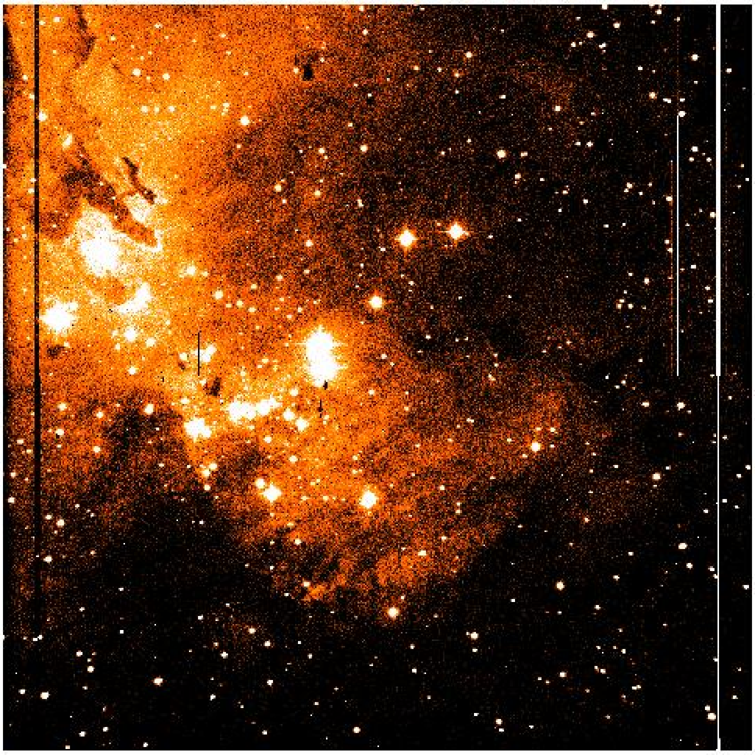

Figure 3.2: Object frame obtained in the B filter; on the left and right edge of the image some bad columns are visible.

Then the stars were selected from the science frames for further analysis. Only stars with an intensity higher than 5 times the sky background and lower than 65535 ADU were selected, to avoid that they are either too faint or saturated, respectively. The complete sample consists of 186 stars. The pixel values of every star were transformed into an x-y- coordinate system, to receive declinations and right ascensions. This allows an easy cross-identification with the star numbers derived from other publications. Figure 3.3 shows the observed field with all selected stars. Those stars out of the selected 186 with a known V magnitude are presented according to their brightness in Figure 3.4. Their known UBV-values are listed in Table 6.2 and in Table 6.3.

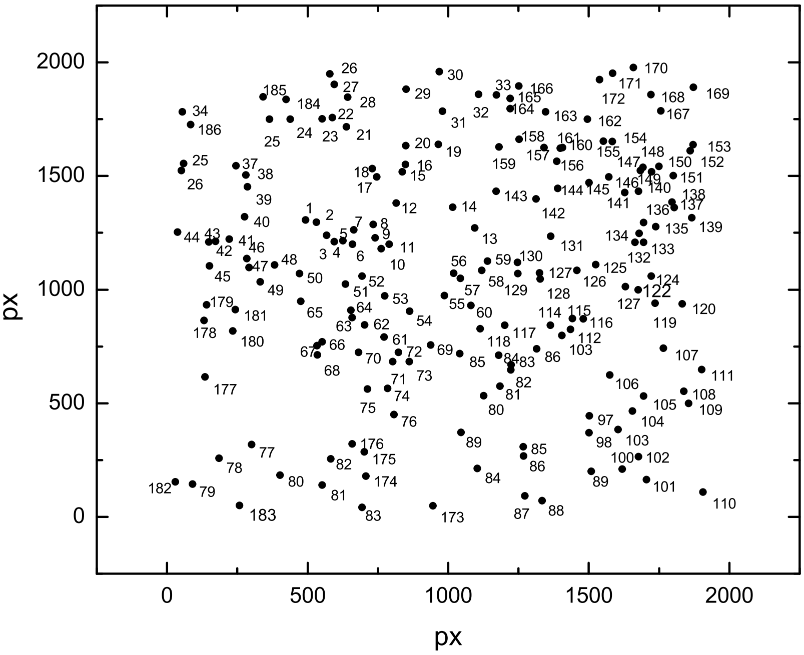

Figure 3.3: Schematic map of the observed field of NGC 6611 with all 186 selected stars. 1 pixel (px) corresponds to 0.369 arcseconds.

3.2.2 Extraction of Lightcurves

For all 186 stars light curves had to be generated using the IDL based tool PODEX (**Ph**O**tometric **D**ata **EX**tractor, Kallinger 2005). Under the aid of this semi-automatic reduction tool, it is possible to extract light curves from photometric time series CCD data. First, all fits files were checked to contain all necessary data, like right ascension and declination of the image center, universal time and integration time of the observations, radius of the aperture of the brightest star used, etc. Bouguer plots (i. e., plots of apparent magnitude versus airmass) helped to determine the individual aperture radii of all stars to receive a minimal point-to-point scatter in the light curves. After defining all demanded data, the light curves were extracted. Because NGC 6611 is a very young cluster embedded in an H II region (Herbig et al. 2001), there is a huge amount of circumstellar dust that might cause variable extinction. Therefore nightly means had to be subtracted to correct for zero point changes and long-term irregular light variations. Furthermore stars in

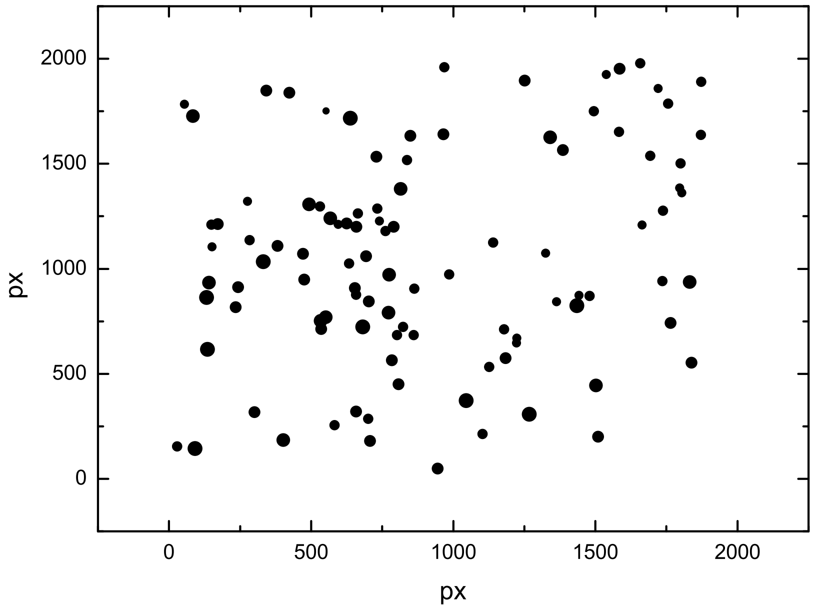

Figure 3.4: Schematic map of those stars with a known V magnitude. 1 pixel (px) corresponds to 0.369 arcseconds. The size of the points corresponds to the brightness of the stars. The magnitudes range from V = 11.29 mag to V = 16.23 mag.

NGC 6611 are known to show an anomalous reddening (Kumar et al. 2004) and an abnormal extinction (Chini et al. 1990). Therefore a color-dependent extinction correction had to be conducted for all instrumental light curves.

3.2.3 Frequency Analysis

The following detailed frequency analysis was carried out using the `Period04` software (Lenz et al., 2005) for both filters. This program is based on classical Fourier techniques. It searches for and fits sinusoidal patterns to time series of data, that show periodic behavior. If a signal exceeds four times the noise level in the amplitude spectrum, it is considered to be significant (Breger et al. 1993 and Kuschnig et al. 1997). After the first frequency analysis, it turned out, that the scatter of the data obtained in the first night was too high. Therefore data from the first night had to be discarded for the further analysis.

A second run of frequency analyses of the selected stars was performed additionally with the program `SigSpec` (SIGnificance SPECtrum, Reegen 2004 and 2007), to confirm the frequencies identified with `Period04`. `SigSpec` also searches for frequencies in time series of stellar photometry and measures their amplitude ratios and peak widths. It computes an amplitude spectrum for a given dataset and significance levels for amplitude spectra of time series. The output contains frequency, amplitude and phase. A signal is treated as significant, when its significance is higher than 5.4575. This corresponds to the significance criterion by Breger et al. (1993), where a peak is treated as real in the amplitude spectrum, when its amplitude signal-to-noise ratio exceeds a value of 4. `SigSpec` yields comparable results to all the frequencies obtained by `Period04`. Only those frequencies, which were significant in both methods, were used for further analysis.

3.3 Results

3.3.1 Pulsating PMS stars in NGC 6611

In the following, own star numbers are used and cross references with the literature are given. Star numbers beginning with W, like W260, correspond to the numbering system of WEBDA. All frequencies and amplitudes measured in both filters with `PERIOD04` are listed in Table 6.4 in the APPENDIX.

Four stars (#7, #71, #82 and #180) out of the selected 186 showed significant pulsation frequencies in the V and B filter, which are listed in Table 3.1. Additionally the astrophysical parameters of all these four new pulsating pre-main sequence stars are listed in Table 3.2. The remaining 182 stars were either inconclusive or constant and need further investigation.

NGC 6611 #7

Hillenbrand et al.(1993) measured a magnitude of V=14.38 mag, a (B-V) of 0.76 mag and an (U-B) of 0.46 mag for star #7 (W260). According to Belikov et al.(1999) the membership probability, that this star belongs to NGC 6611, is 20 %.

The frequency analysis showed one single significant pulsation frequency at 25.15 c/d, corresponding to 57.3 minutes with an amplitude of 2.8 mmag in V, and 3.4 mmag in B. The amplitude spectrum in both filters can be seen in Figure 3.5 and in Figure 3.6. Figure 3.7 shows the differential light curves in the V and B filter. An offset of 0.02 in the y direction was applied to B mag for better visibility.

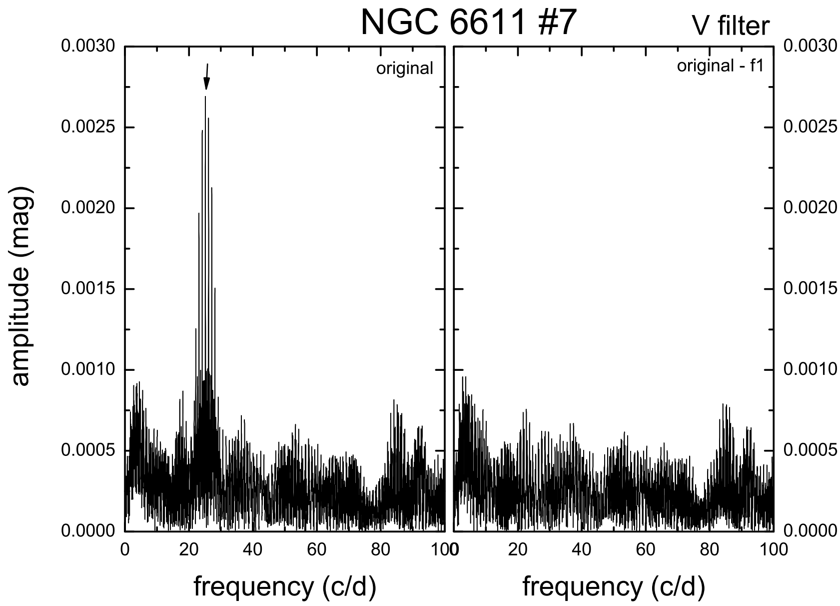

Figure 3.5: Amplitude spectrum of NGC 6611 #7 in the V filter, where the identified frequency is marked with an arrow. The right panel shows the residual amplitude spectrum after prewhitening.

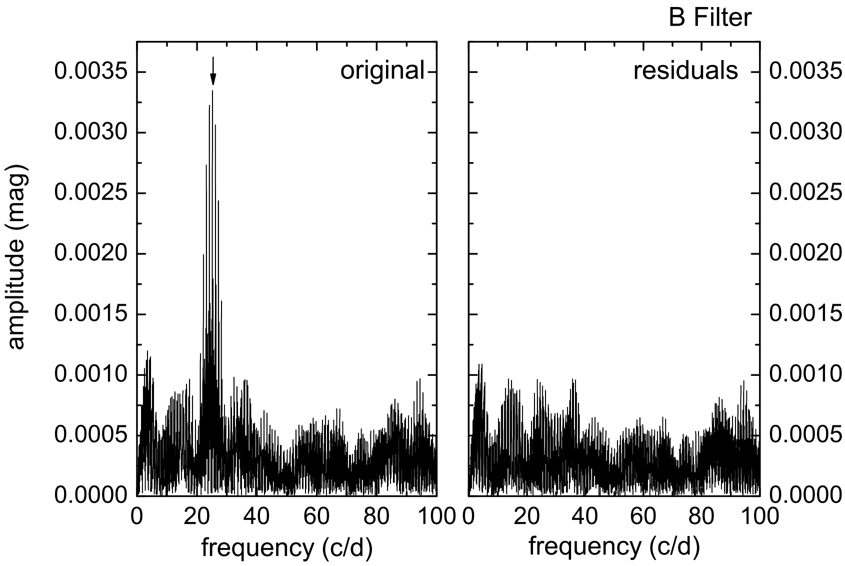

Figure 3.6: Amplitude spectrum of NGC 6611 #7 in the B filter, where the identified frequency is marked with an arrow. The right panel shows the residual amplitude spectrum after prewhitening.

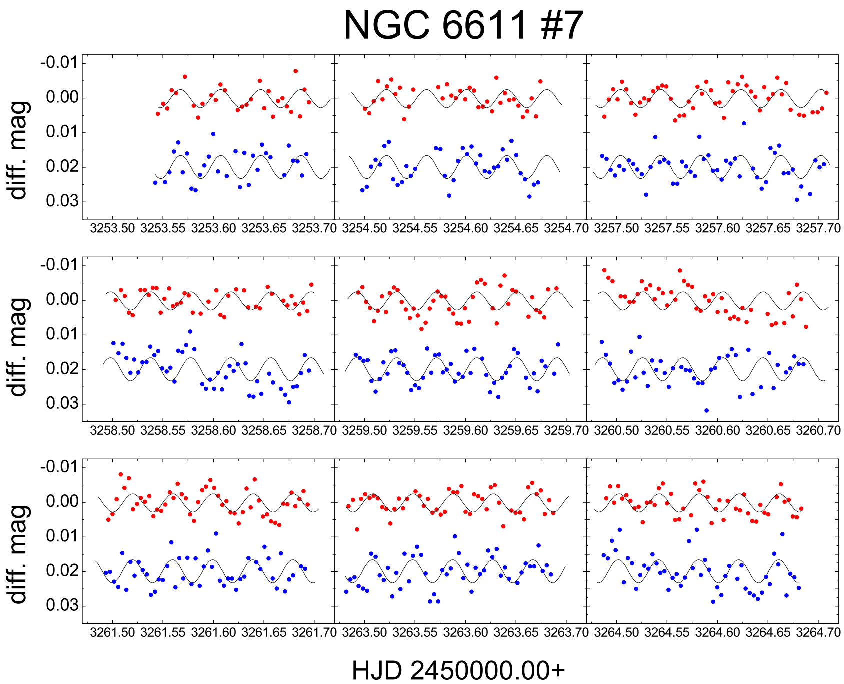

Figure 3.7: Differential light curves of NGC 6611 #7; top: V filter, bottom: B filter shifted in Y-direction for better visibility. The multi-sine fit with one frequency is represented by the solid line.

NGC 6611 #71

Star #71 (W221) has a V of 14.55 mag, shows a (B-V) of 1.02 mag and an (U-B) of 0.62 mag (Hillenbrand et al.1993). Its membership probability is 89% according to Belikov et al.(1999). Hillenbrand et al.(1993) also classified the star to be of B8Ve spectral type. In their studies the authors detected a large number of emission line stars among their observed stars with a spectral type later than B1. The emission appeared within the cores of the Balmer absorption lines. They considered the emission line of NGC 6611 #71 as a result of interaction with a sorrounding circumstellar disk and the embedding of the cluster into the Eagle nebula. The region of this star is highly reddened and an anomalous extinction law could be observed. Therefore star #71 appears redder than expected. Also Chini and Wargau (1990) confirmed this abnormal extinction. All early type stars in NGC 6611 are highly influenced by the amount of dust originating from the nearby H II region. Stars of later spectral type ($\geq$ B5) follow a normal reddening path.

The analysis of the lightcurve showed one single significant frequency of 9.32 c/d, that corresponds to 2.58 hours with an amplitude of 10.1 mmag in V, and 13.4 mmag in B. Figure 3.8 shows the amplitude spectrum in V and Figure 3.9 in B. The differential light curves are presented in Figure 3.10. The B mag light curve was plotted with an offset of 0.02 for better visibility.

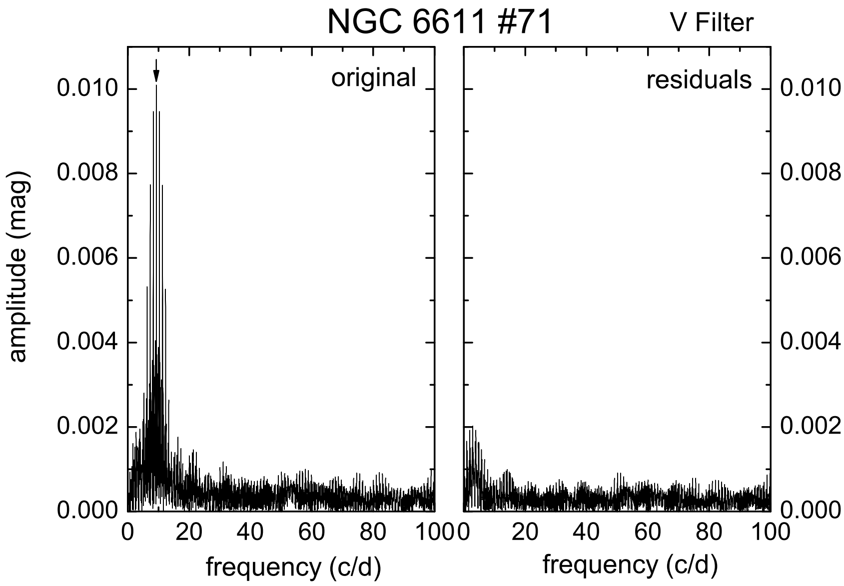

Figure 3.8: Amplitude spectrum of NGC 6611 #71 in the V filter, where the identified frequency is marked with an arrow. The right panel shows the residual amplitude spectrum after prewhitening.

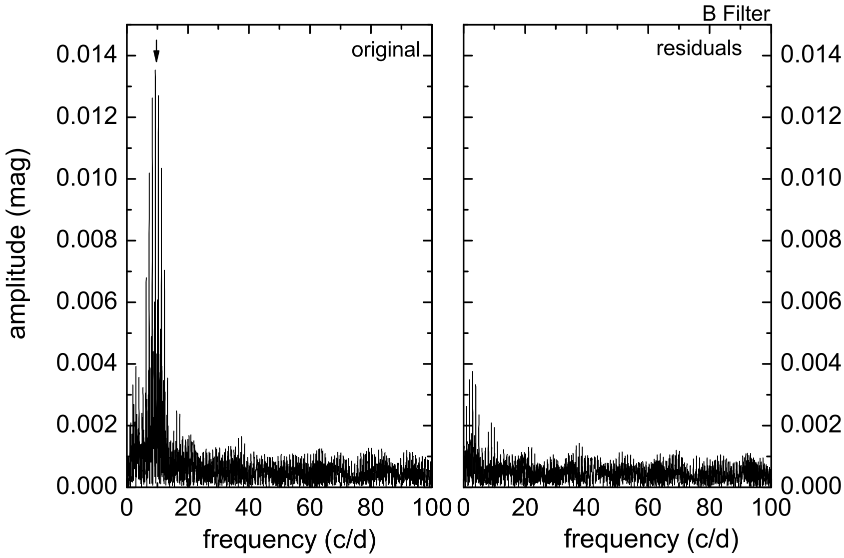

Figure 3.9: Amplitude spectrum of NGC 6611 #71 in the B filter, where the identified frequency is marked with an arrow. The right panel shows the residual amplitude spectrum after prewhitening.

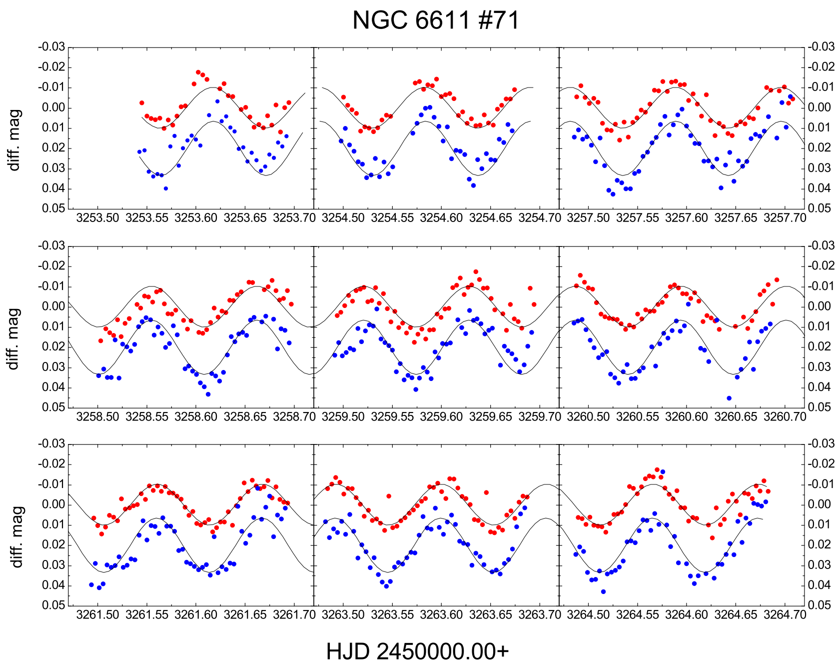

Figure 3.10: Differential light curves of NGC 6611 #71; top: V filter, bottom: B filter shifted with an offset of 0.02 in Y-direction for better visibility.

NGC 6611 #82

CCD observations of Hillenbrand et al. (1993) obtained for the star #82 (W292) a V magnitude of 14.09, a (B-V) of 0.78 mag and an (U-B) of 0.41 mag. There are two opinions concerning the membership probability of this star repeated in the literature. According to Belikov et al. (1999) the probability lies at 84 %. Tucholke et al. showed in 1986 that it should be only about 29%.

Belikov et al. (1999) based their measurements for the membership probabilities on spatial and proper motion distributions of stars in this region. For the reliability they used a statistical method (Kharchenko et al., 1995), based on the information of proper motions and positions of stars in the cluster neighbourhood. A star like #82, with a membership probability of 84%, is located at a distance less than 1σ from the maximum of the distribution function.

The determination of the membership probability according to Tucholke et al. (1986), applied the proper motion distribution as a sum of a two-dimensional Gaussian for cluster stars and an approximately constant background of field stars. Their error limit varies between the amount of stars agreeing to the distribution calculations and stars with small proper motion errors.

For star #82 three pulsation frequencies were discovered. The first one is at 29.876 c/d, corresponding to 48.2 minutes with an amplitude of 2.2 mmag in V and 3.28 mmag in B. The second frequency is at 25.697 c/d, corresponding to 56.04 minutes, with an amplitude of 1.78 mmag in V and 2.02 mmag in B. The third frequency lies at 23.19 c/d, corresponding to 1.03 hours with an amplitude of 1.3 mmag in V and 1.5 mmag in B. The amplitude spectrum of both filters can be seen in Figure 3.11 and Figure 3.12. The differential light curves are shown in Figure 3.13.

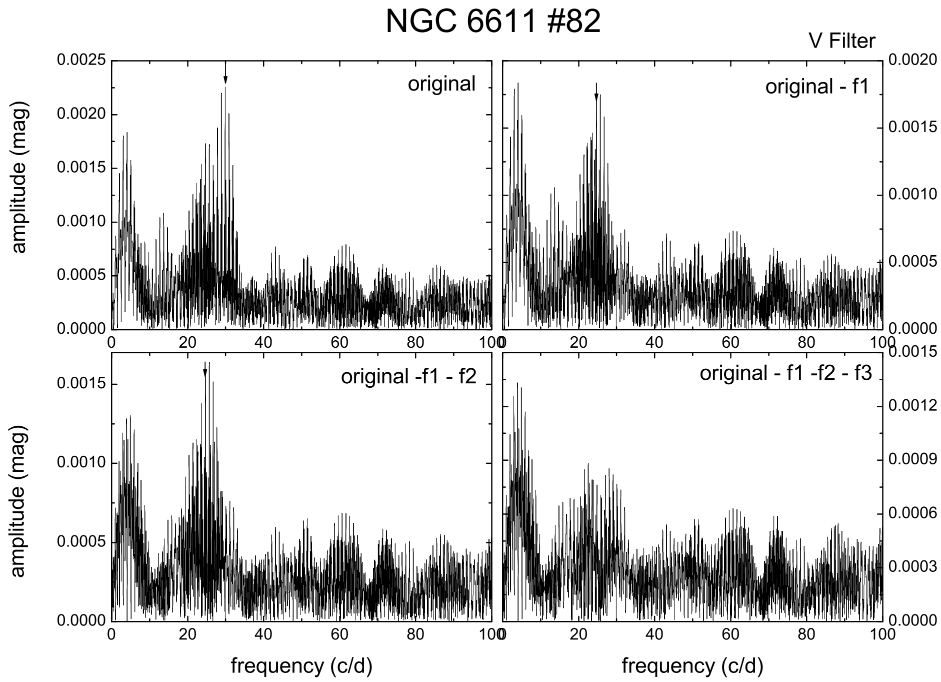

Figure 3.11: Amplitude spectra of NGC 6611 #82 in the V filter, where the identified frequencies are marked with arrows.

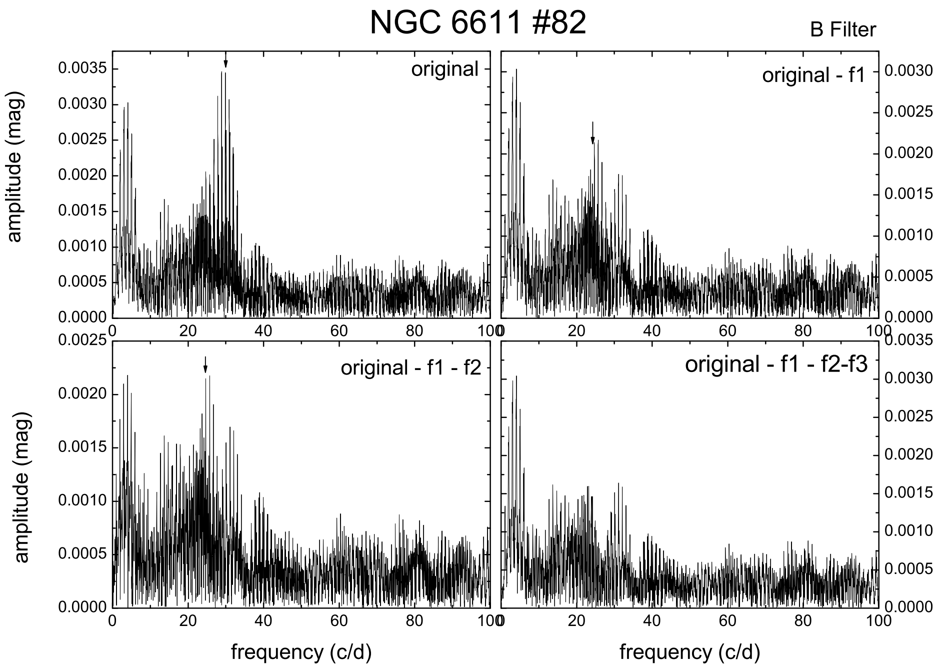

Figure 3.12: Amplitude spectra of NGC 6611 #82 in the B filter, where the identified frequencies are marked with arrows.

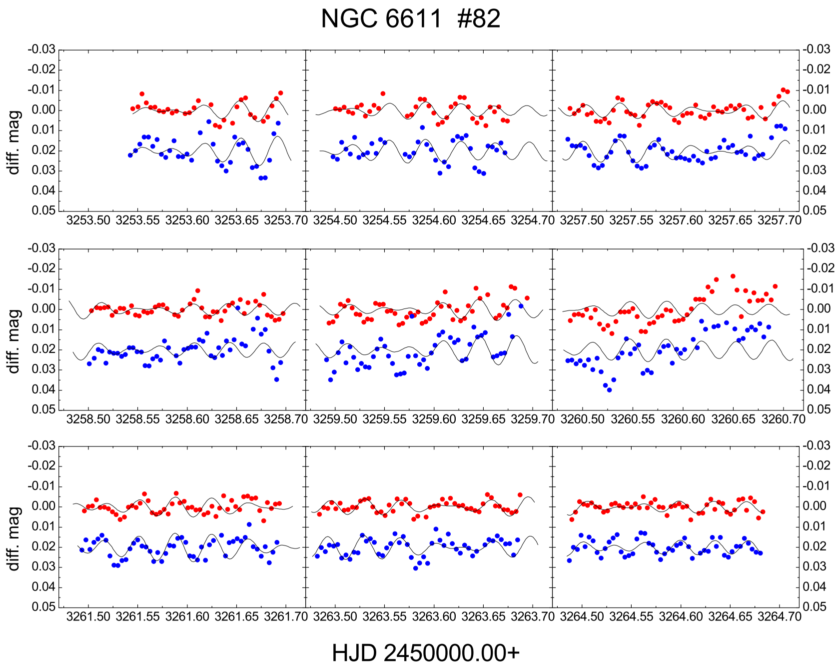

Figure 3.13: Differential light curves of NGC 6611 82; top: V filter; bottom: B filter plotted with an offset of 0.02 for better visibility.

NGC 6611 #180

According to Chini et al. (1990) star #180 (W374) has V=13.02 mag, (B-V)=0.95 mag and (U-B)=0.28 mag. They did not observe any abnormal reddening and mentioned no influence by the surrounding dust. Together with proper motion studies Chini et al. (1990) classified this star as a foreground object. They also considered the possibility that the star is located at the front edge of the cluster. Corresponding to its position in the HRD, #180 seems to be a PMS star, but the membership to the cluster is unclear. Belikov et al.(1999) calculated a membership probability of only 4 %. Also Tucholke et al.(1986) confirmed, based on their observations, that this star is not a member of the cluster NGC 6611. Proper motion studies performed by de Winter et al. (1991) also yielded a low membership probability of this star to NGC 6611, but they detected an E(B-V) larger than 0.5 mag, which is the value for the foreground excess of NGC 6611. So it seems to be located in the cluster region but not belonging to the cluster. De Winter et al. (1997) classified the star to be of spectral type F2e. In their opinion star #180 is a boundary case concerning its membership to the cluster, because it shows a E(B-V) value of $0^{m}.56$, has a position close to the stellar birthline and it seems to be surrounded by dust. According to Winter et al. (1997) a star is a cluster member when its E(B-V) value is larger than $0^{m}.50$. It therefore seems to be an ideal candidate for a pre-main sequence star.

The frequency analysis of the light curves of #180 showed a multi-periodicity consisting of 6 significant frequencies. The observed frequencies lie between 5.15 c/d and 13.3 c/d. They span a period range between 1.8 hour to 4.65 hours with amplitudes from about 2 mmag to 14.8 mmag. Figure 3.14 shows the amplitude spectra in the V filter and Figure 3.15 in the B filter. The differential light curves in both filters are presented in Figure 3.16.

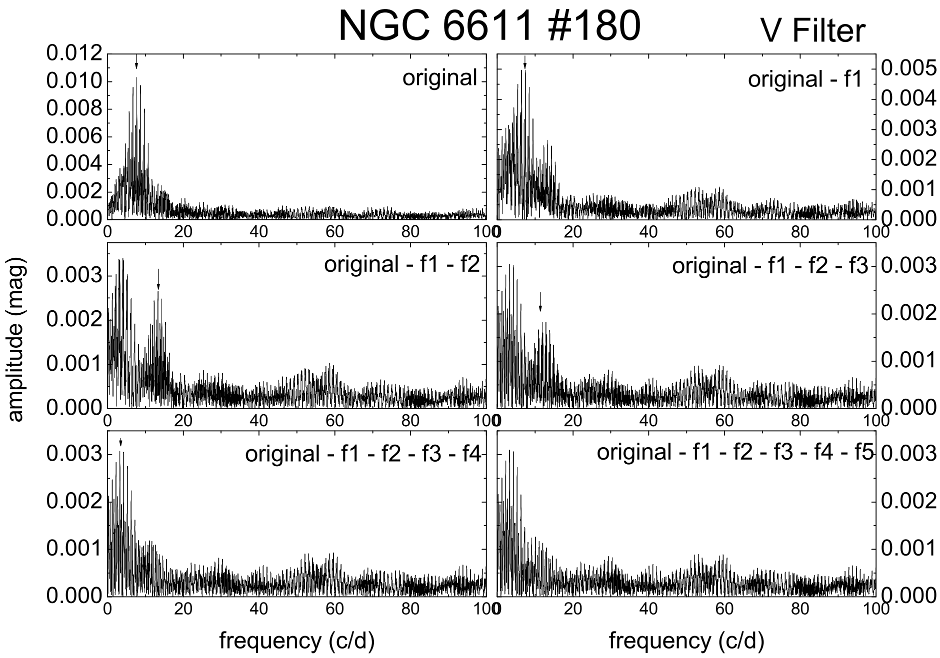

Figure 3.14: Amplitude spectra of NGC 6611 #180 in the V filter, where the identified frequencies are marked with arrows.

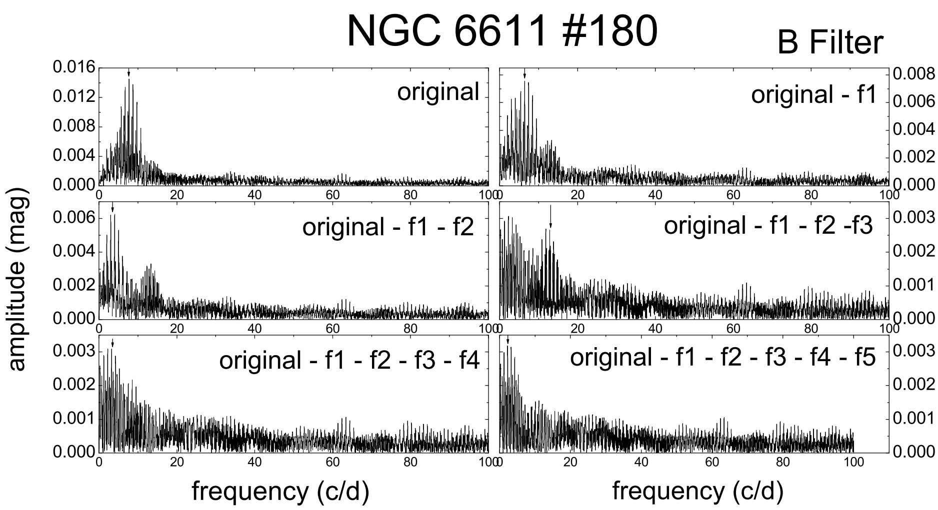

Figure 3.15: Amplitude spectra of NGC 6611 #180 in the B filter, the identified frequencies are marked with arrows.

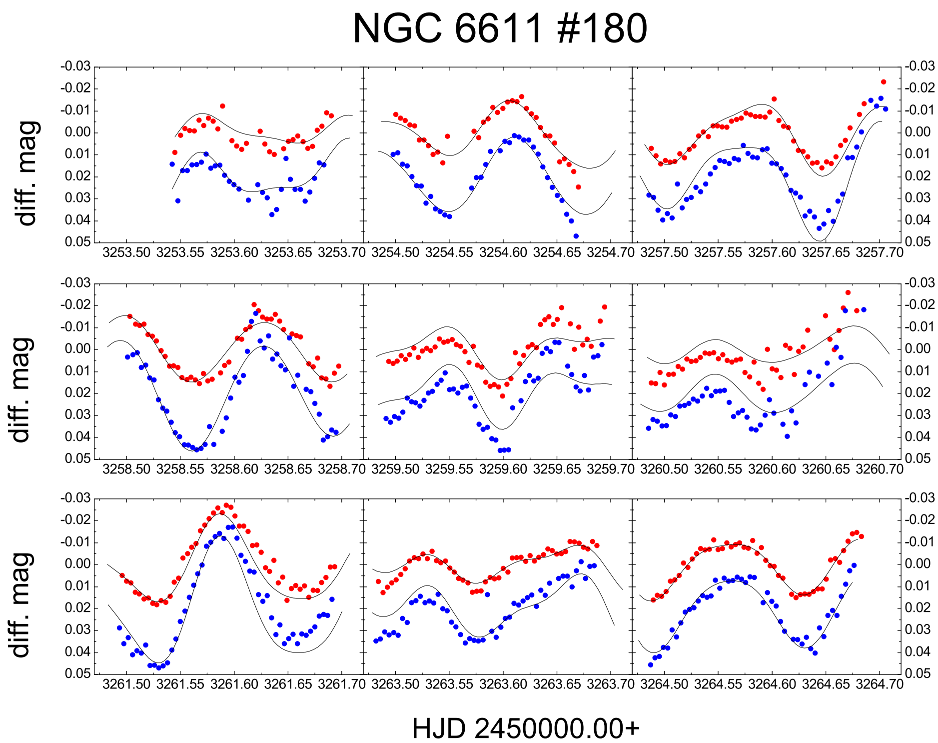

Figure 3.16: Differential light curves of NGC 6611 180; top: V filter; bottom: B filter shifted for better visibility with an offset of 0.02.

3.3.2 Summary of pulsating PMS stars in NGC 6611

According to these observations, the total number of pulsating pre-main sequence stars increases by four. Two stars (#7, #71) were monoperiodic and two stars (#82, #180) were multiperiodic in the present data. Among the remaining 182 stars no other pulsators or variable stars could be detected. Three stars #60 (W153), #96 (W111) and #132 (W53), were inconclusive and would need further investigations and observations concerning their variability. The identified frequencies of the four new pulsators and their astrophysical parameters are listed in Table 3.1 and Table 3.2.

star	Webda	filter	No #	freq. [c/d]	amp. [mag]	phase	noise [mag]	S/N
7	260	V	1	25.148	0.003	0.575	0.0002	10.132
71	221	V	1	9.316	0.010	0.171	0.0003	32.08
82	292	V	1	29.876	0.002	0.368	0.0002	7.947
		V	2	25.697	0.002	0.289	0.0003	5.384
		V	3	23.189	0.001	0.254	0.0003	5.555
		V	4	12.692	0.001	0.747	0.0001	5.274
		V	5	21.510	0.001	0.819	0.0002	4.192
180	374	V	1	7.739	0.011	0.192	0.0004	25.559
		V	2	6.436	0.006	0.951	0.0005	9.651
		V	3	13.335	0.003	0.029	0.0004	5.717
		V	4	12.875	0.002	0.539	0.0004	4.688
		V	5	8.526	0.01	0.514	0.0004	3.215
		V	6	5.158	0.002	0.708	0.001	2.397
7	260	B	1	25.151	0.003	0.047	0.0004	8.173
71	221	B	1	9.317	0.013	0.348	0.0004	28.358
82	292	B	1	28.870	0.003	0.324	0.0004	8.081
		B	2	25.699	0.002	0.568	0.0003	5.355
		B	3	31.086	0.002	0.459	0.0003	5.092
		B	4	13.716	0.002	0.904	0.0004	3.793
		B	5	23.193	0.002	0.449	0.001	2.580
180	374	B	1	7.736	0.015	0.046	0.0004	32.930
		B	2	6.433	0.008	0.338	0.001	15.098
		B	3	13.338	0.003	0.062	0.001	4.783
		B	4	12.860	0.003	0.633	0.001	4.651
		B	5	8.518	0.003	0.277	0.0004	4.943
		B	6	5.244	0.003	0.899	0.001	3.998

Table 3.1: Identified pulsation frequencies of the four pulsating stars in both filters. The upper part lists the frequencies found in the V-filter data. Below are those of the B-Filter.

star	Webda	V [mag]	(B-V) [mag]	(U-B) [mag]	sp
7	260	14.4	0.76	0.46	
71	221	14.55	1.02	0.62	B8 Ve
82	292	14.1	0.78	0.41	
180	374	13.41	0.91	0.82	F2 e

Table 3.2: Astrophysical parameters of the four discovered candidates for PMS pulsation in NGC 6611. UBV values are taken from Hillenbrand et al. (1993).

Chapter 4

Spectroscopic observations of stars in NGC 6611, NGC 6530 and NGC 6383

Spectroscopy, i.e. the dispersion of the light into different wavelengths, includes a lot of information about the physical nature of the stars. Depending on the energy distribution level, light is absorbed or emitted and either absorption, or emission lines or both are getting visible within stellar spectra. One of the goals of stellar atmosphere studies is to understand the varied profiles and line strengths shown by stars (Gray 1992). Another is to use our knowledge of line behavior to interpret the fundamental properties of stars, for example, the measurement of effective temperature, surface gravity, radii and chemical composition.

According to the temperature of a star different characteristic lines are getting visible. Whereas for example He I and He II lines are typical for hot stars, stars of lower temperatures contain a lot of metallic lines, like Fe I. Some of the temperature sensitive lines like the hydrogen Balmer series, can be used to get an estimate for the effective temperature of a star. Moreover line depths and widths can be used to derive surface gravities and $v \cdot \sin i$ values.

For most of the pulsating pre-main sequence stars observed in this work, neither spectral classes nor fundamental parameters are available in the literature. Information about the spectral type or effective temperature are important to put the star into the correct position in the HR-diagram. Within this work pulsating pre-main sequence stars of the three clusters NGC 6611, NGC 6383 and NGC 6530 were analyzed spectroscopically. The aim was getting additional information about the stars for their further interpretation, i. e. the determination of effective temperatures and gravities. Pulsating pre-main sequence stars are known to show a lot of emission lines within the hydrogen Balmer series, Fe I or Ca II. Also variations in the line profiles of Hα from single to double peak emissions are known (Vieira et al., 2003). The obtained spectra should help to determine the position of the discovered variable stars in the HR diagram and give additional information for their asteroseismic analysis.

4.1 Observations

Spectroscopic observations of several selected pulsating pre-main sequence stars in the three young clusters NGC 6611, NGC 6530 and NGC 6383, have been obtained additionally to already existing photometric observations. The selection of the target stars depended on previous photometric studies (this work and Zwintz 2005).

Classification spectra of the variable stars in all three young clusters were observed with the R-C spectrograph at the CTIO 1.5 m telescope during an observational period that lasted from March 2007 to July 2007. The wavelength range is from 4050 Å to 4700 Å. This range includes the typical lines, like the Hydrogen Balmer series, Ca II, Fe I, Mg II, for the classification of A and F type stars. The magnitude range of the observed stars lies between V=10 mag and V=16 mag.

Due to the faintness of the target stars, several short exposures per star were taken during same nights, allowing the combination of the object frames to receive a better signal to noise ratio. Table 4.1 lists the targets for spectroscopic observations and analysis.

In addition to the object frames several bias frames, flat-field images and HeAr arc lamp exposures for wavelength-calibration were taken.

4.2 Data reduction

4.2.1 CCD reduction

All images are stored in the FITS-format. The reduction steps have been done using the software package `IRAF`. Each night 25 bias frames were taken. A masterbias was created using the IRAF-task `zerocombine` in the `noao - imred - ccdred` package. The resulting frame was subtracted from all flat-field, arc and science frames using the `ccdproc` task.

To remove all the pixel-to-pixel variations across the CCD chip, the obtained flat-field exposures were used. 25 flat-field images (an example is given

Object	ID	α(2000.0)	δ(2000.0)	V(mag)	Exp. time	N of exp.
NGC 6383	W55	17:34:48.0	-32:37:24.0	12.8	360	4
NGC 6383	W54	17:34:55.0	-32:35:30.9	12.3	360	3
NGC 6383	W262	17:34:39.6	-32:34:10.9	12.8	360	4
NGC 6530	W159	18:04:42.3	-24:18:03.5	14.7	480	6
NGC 6530	W78	18:04:30.8	-24:23:42.1	12.4	600	8
NGC 6530	W53	18:04:20.7	-24:24:55.7	12.4	360	5
NGC 6530	W57	18:04:21.8	-24:15:46.9	10.7	600	7
NGC 6530	W161	18:04:20.8	-24:14:05.2	17.0	600	7
NGC 6530	W38	18:04:13.9	-24:13:28.0	13.6	300	3
NGC 6530	W94	18:04:37.6	-24:21:11.6	12.5	360	3
NGC 6530	W75	18:04:28.6	-24:18:56.5	9.8	600	8
NGC 6530	W114	18:04:50.6	-24:25:42.0	15.9	300	3
NGC 6611	W260	18:18:41.4	-13:49:05.0	14.4	600	10
NGC 6611	W292	18:18:43.7	-13:42:20.7	14.1	600	8
NGC 6611	W110	18:18:23.0	-13:41:07.3	14.5	600	10
NGC 6611	W43	18:18:13.2	-13:50:53.7	14.5	600	10
NGC 6611	W41	18:18:11.9	-13:46:55.6	14.2	600	8
NGC 6611	W221	18:18:37.6	-13:45:12.6	14.6	600	10

Table 4.1: Target table for spectral classification; the W numbers correspond to the WEBDA numbering system.

in Figure 4.1) were taken each night. Using the IRAF-task `flatcombine` the single flat-field exposures were combined to create a masterflat image.

Before the flat-field division could be performed, a normalization process has to be conducted. Figure 4.2 shows, that the CCD chip has no uniform illumination level. Large scale variations are visible all over the chip. To get rid of these variations and possible colouring effects of the flat-field lamp, all combined flat-field images were normalized and fit by a low order polynomial with the `imsurfit` and the `response` tasks within the `noao - twodspec - longslit` package. One of the obtained results can be seen in Figure 4.3. Only the unrepairable effects on the CCD, like hot pixels and bad columns, as seen in Figure 4.4, are remaining on the normalized flat-field.

After these steps all comparison and science frames could be divided by the normalized masterflat.

4.2.2 Extraction of the spectra and wavelength calibration

The `apextract` package includes all necessary routines for extracting the spectra. First the object frames have to be analysed. In order to derive the position of the spectra and to define the dispersion axis, the `implot` task is used. With a cut perpendicular to the dispersion axis, the location of the

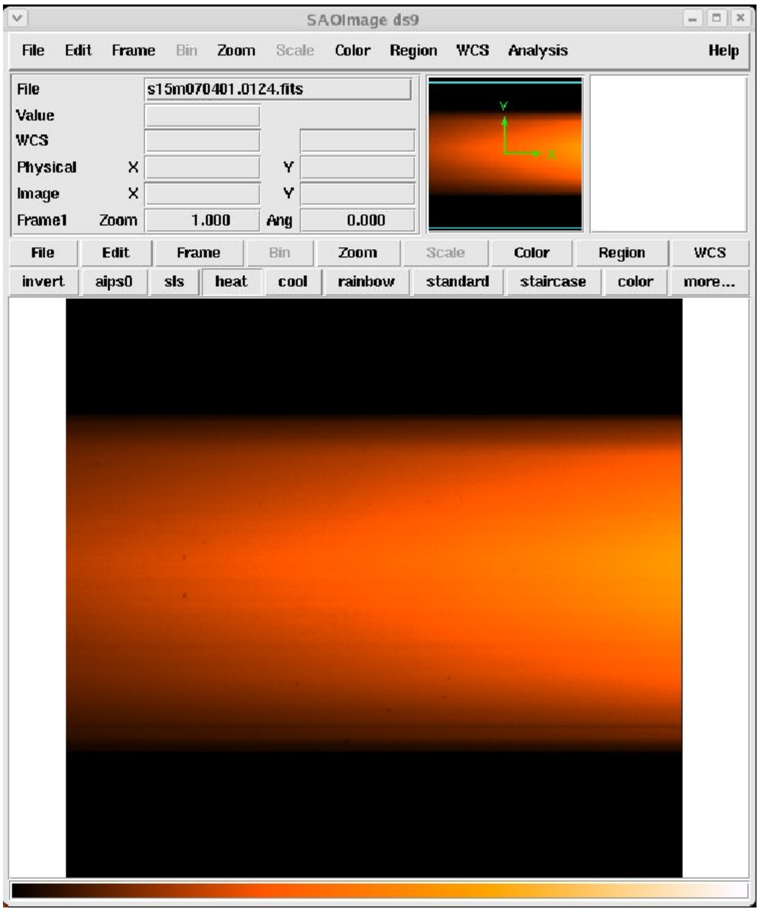

Figure 4.1: Example for a flat-field image, coloured by the heat color table

spectral profile is determined. Afterwards the `apall` procedure allows in a multi-step task to extract the spectrum. Following this extraction, the He-Ar arc spectrum with the identical centering and trace has to be extracted, using `apall` again. Finally the wavelength calibration had to be performed using `identify`. Figure 4.5 shows one step of the wavelength identification process, which is based on the CTIO linelist for the He-Ar comparison lamps. The use of the task `dispcor` provides every object frame with the same wavelength scale.

The last two reduction steps consist in the heliocentric and radial velocity corrections of all object spectra. The tasks used are `rvcorrect` and `dopcor` in the `noao - astutil` package. To receive a better signal to noise ratio, the science frames of the same objects were combined.

Then the continuum was fitted and normalized. The continuum fitting was performed under the aid of the IDL program `dvd2dat.pro` (Spectral

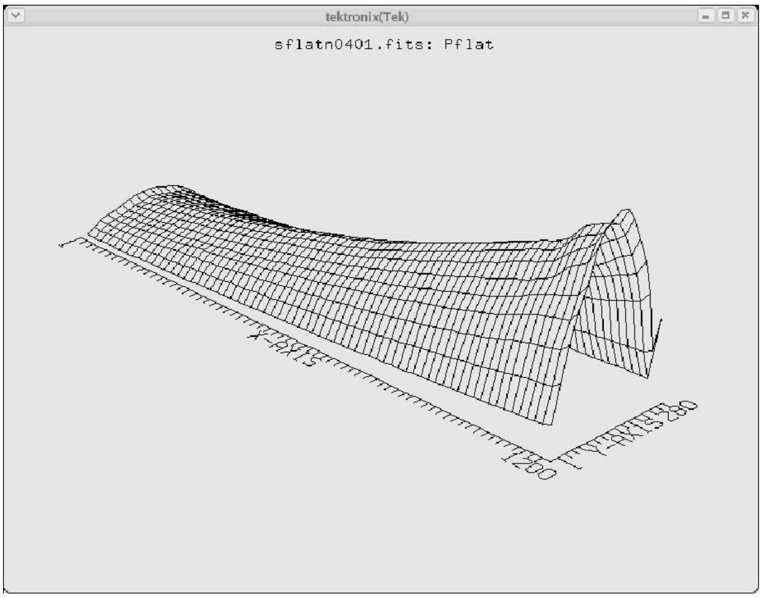

Figure 4.2: Surface plot of the combined flat-field illustrating the non-uniform illumination level.

normalization IDL, Kochukhov, priv. comm.). Low order polynomials with orders from 3 to 8 were used for normalization. Especially the lines of the Hydrogen-Balmer series are for A and F type stars very sensitive to temperature and pressure (Gray 1992). Therefore the lines Hδ and Hγ were treated with special attention to keep their characteristics, like the depth and width of the wings, which are important for the later determination of effective temperature.

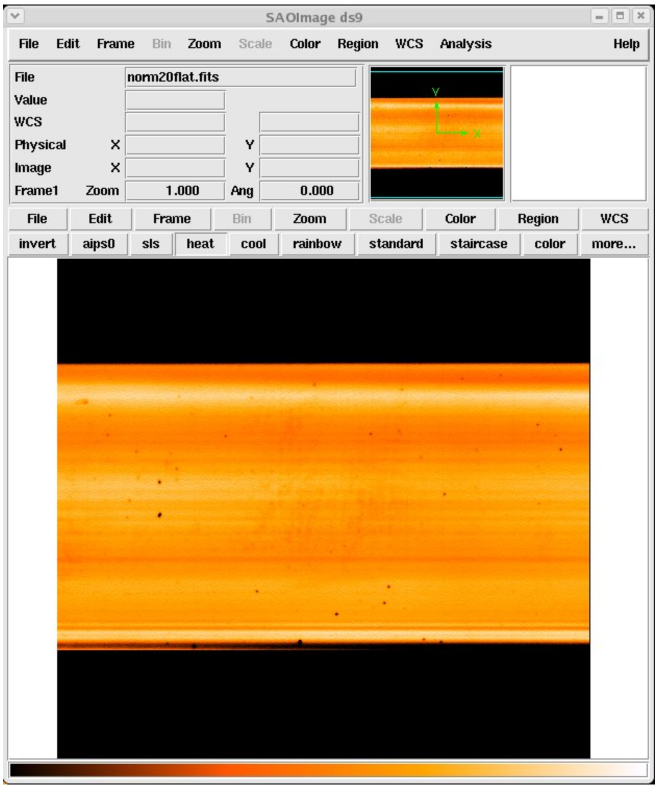

Figure 4.3: Plot of the normalized flat-field image, coloured by the heat color table

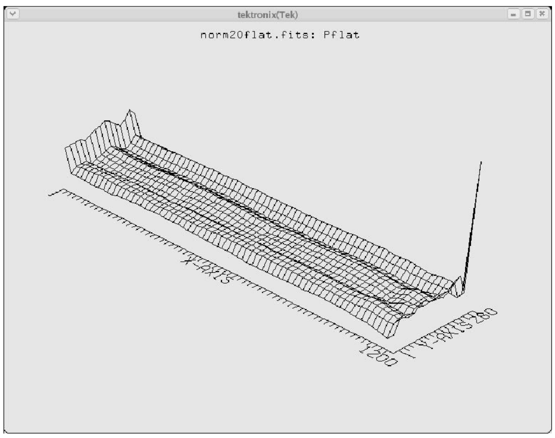

Figure 4.4: Surface plot of the normalized flat-field; on the edges some hot pixels are visible

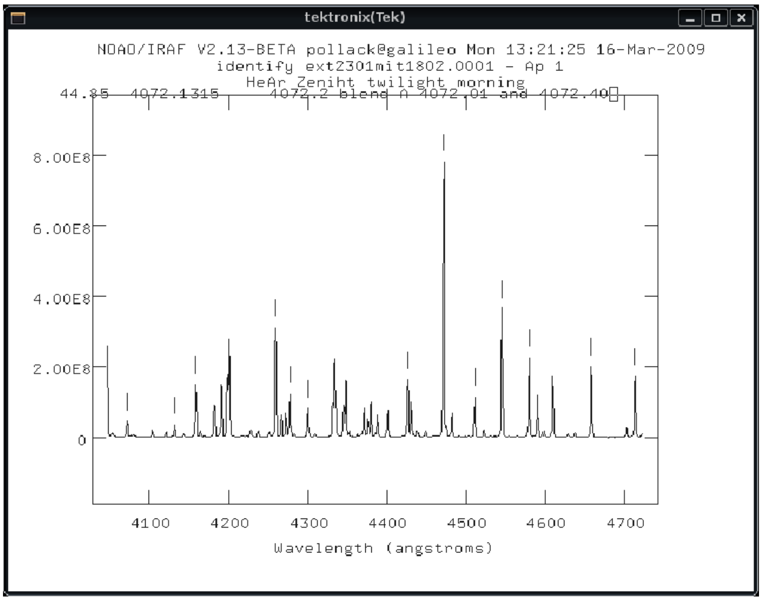

Figure 4.5: Identification of the wavelengths. The marked lines are those which correspond to the CTIO linelist.

4.2.3 Determination of fundamental parameters

Once the spectra were extracted and normalized, the resolution of the spectra was calculated to prove the resolution of the spectrograph and to get the analysing programs adjusted. The spectra were plotted and the FWHM of several lines were measured. Figure 4.6 shows the measured FWHMs. The mean of the wavelengths and the mean of the FWHMs were calculated and under the aid of the formula: $R = \lambda/\Delta\lambda$ the resolution was determined. The resolution of the spectra is $R = 2980.86 \pm 270.4$ Å and corresponds well to the value of R = 2845 Å given for the spectrograph. Then the determination of the fundamental parameters could be started. For getting an estimate of the effective temperature, the spectra were compared with model grids calculated with `ATLAS9` (Kurucz 2005). `ATLAS9` calculates grids of model atmospheres for a temperature range from 3500 K to 50 000 K, and for a log g range from 0.0 to 5.0. Several model atmospheres in the wavelength range from 6000 K to 9000 K, which are typical for A and F type stars, were calculated in combination with the `Abundance Analysis Procedure` (AAP; Gelbmann et al. 1997). This script extracts atomic line data from `VALD` (Vienna Atomic Line Database, Piskunov et al. 1995) and calculates synthetic spectra. Using `ROTATE` (Piskunov et al. 1998, updated by Michael Gruberbauer) the observed spectra were compared with the calculated models.

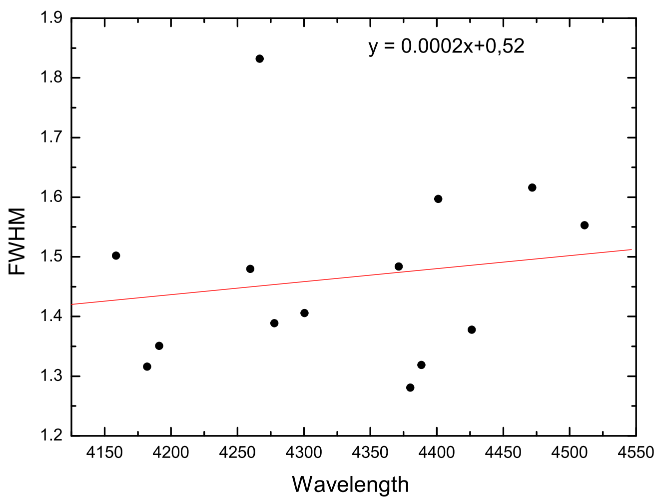

Figure 4.6: This figure shows the measured FWHMs for the determination of the resolution of the spectra. The red line is a regression to the data.

There are differences in the shape of absorption lines, the content of elements and sometimes emission lines, comparing stellar spectra. These different shapes of lines depend for example on temperature, pressure and rotation. All computed models are based on the assumption of a local thermal equilibrium (LTE). That means that the interactions between gas and radiation are based on pure absorption. These models will offer good estimates for the fundamental parameters of the A and F type stars. LTE based model calculations might cause problems in really hot stars, like O stars, where the radiation dominates over the collisional interactions. In those cases non-LTE models would present better approximations, but they are currently still under development (Gray 1992).

The determination of the effective temperature was based on the comparison of the stellar profile of the Hδ and Hγ lines with a synthetic spectrum. The strength of a line is a function of the temperature. For the estimate of the effective temperature, the shape of the wings and the strength of the lines were used. Because of the pressure sensitivity of the hydrogen lines in the range of A and F type stars additional information was taken into account, like He I and He II lines, that only appear in hotter stars. For lower temperatures, e.g. in the range of late F type stars, the G-Band gets visible. The G-band appears as a damp within a spectrum in the wavelength range from $\lambda = 4295$ to 4315 Å, which consists of many spectral lines of the CH-molecule and can therefore be used as an indicator for lower temperatures (Shelyag et al., 2004).

To estimate the surface gravity, model atmospheres with different log g values were calculated. The surface gravity influences the broadening of the lines. Therefore it is important to use unblended lines. In this data there were hardly no unblended lines, which made the determination of the log g very difficult. Mainly the hydrogen lines were used again. The determinations were based on a log g of 4, which fitted quite well the shape of the stellar spectra.

To make the determination of the $v \cdot \sin i$ values possible, the line profile of the star has to be compared with the synthetic spectrum. The reference lines should be free of broadening effects caused by pressure, should be strong enough to allow any measurements and should be unblended. In the hot stars the lines of He I ($\lambda = 4388$ Å and $\lambda = 4471$ Å) were used. Also the Mg II line ($\lambda = 4481$ Å) in the B and A type stars was used. Additionally the Fe I lines ($\lambda = 4473$ Å and $\lambda = 4476$ Å) can be used. An abundance analysis was not possible using the present low-resolution data due to the lack of resolved and unblended lines.

4.3 Observational results

4.3.1 NGC 6383

NGC 6383 is a very young cluster that is not associated with a star-forming region (Thé et al. 1985). Photometric investigations performed by Thé showed no H_α- emission objects. Lloyd Evans (1978) found a small amount of faint variable stars in this cluster. Spectra of three stars W54, W55 and W262 belonging to the cluster NGC 6383 were obtained and analysed in this work. All three observed stars showed no emission lines.

NGC 6383 W54

According to Lloyd Evans (1978), NGC 6383 W54 has a Johnson V = 12.29 mag, a (B-V) = 0.590 mag and an (U-B) = 0.1 mag. It is a suspected PMS pulsator (Zwintz et al. 2005). Spectroscopic analyses of Thé et al. (1985) defined a spectral class of F0Ve for this star. But his model calculations showed a discrepancy between the effective temperatures of 6500 K and 7500 K.

Figure 4.7 shows the calculated model atmosphere with an effective temperature of 6500 ± 300 K, a log g of 4.0 ± 0.5 and a $v \cdot \sin i$ of 80 ± 30 km/s. The comparison of the calculated synthetic spectrum (red) with the observed spectrum (black) showed that this temperature fits the observations quite well. There was no good fit using a synthetic spectrum with 7500 K. No emission lines were found in the spectrum. The apparent emission line at $\lambda = 4550$ Å and the strong absorption feature at $\lambda = 4180$ Å are reductional artifacts.

NGC 6383 W55

NGC 6383 W55 has a V of 12.8 mag, a (B-V) of 0.65 mag, an (U-B) of 0.44 mag (Lloyd Evans 1978). It clearly shows δ Scuti-like pulsation (Zwintz et al. 2005). No spectral classification is available in the literature for this star, but an effective temperature of 7345 K was determined from Johnson V and (B-V) values (Kenyon et al. 1995). Using our observed spectra we obtain an effective temperature of 6900 ± 300 K, a log g of 4.0 ± 0.5 and a $v \cdot \sin i$ of 25 ± 25 km/s. The $v \cdot \sin i$ value is so small if any, that it was not better detectable because of the low resolution spectra. No emission lines were visible within the spectrum. Figure 4.8 shows the strong lines Hδ and Hγ in absorption.

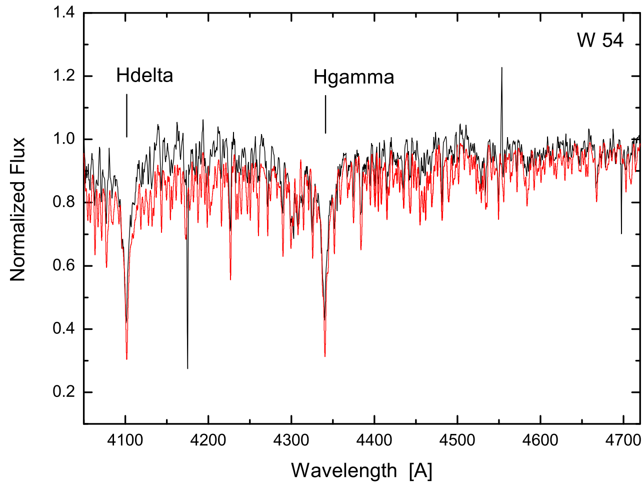

Figure 4.7: Comparison between the observed (black) and the synthetic spectrum (red) of W54 with a T_{eff} of 6500 K, log g of 4.0 and a $v \cdot \sin i$ of 80 km/s. The apparent emission line is a reductional artifact.

NGC 6383 W262

Fitzgerald et al. (1978) derived a V of 12.82 mag, a (B-V) of 0.32 mag and an (U-B) of 0.190 mag of NGC 6383 W262. It is a variable star, but it is inconclusive, if it is a PMS pulsator or not (Zwintz et al 2005). Also for this star there was no spectral classification available in the literature. Model calculations showed that this star has an effective temperature of 6500 $\pm$ 300 K with a log g of 4.0 $\pm$ 0.5 and a $v \cdot \sin i$ of 100 $\pm$ 20 km/s. Within the spectrum the G-band, a damp in the spectrum in the wavelength range from λ = 4295 to 4315 Å which is characteristic for stars cooler than 6000 K is visible, but there were no emission lines. It was not possible to get a good fit for both hydrogen lines. Either Hδ or Hγ could be modeled. Figure 4.9 shows the comparison between the observed and the synthetic model.

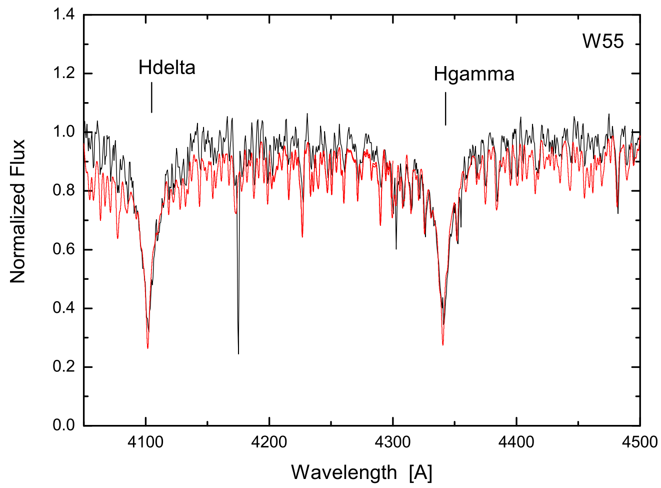

Figure 4.8: Comparison between the observed (black) and the synthetic spectrum (red) of W55 with a T_{eff} of 6900 K, log g of 4.0 and a $v \cdot \sin i$ of 25 km/s.

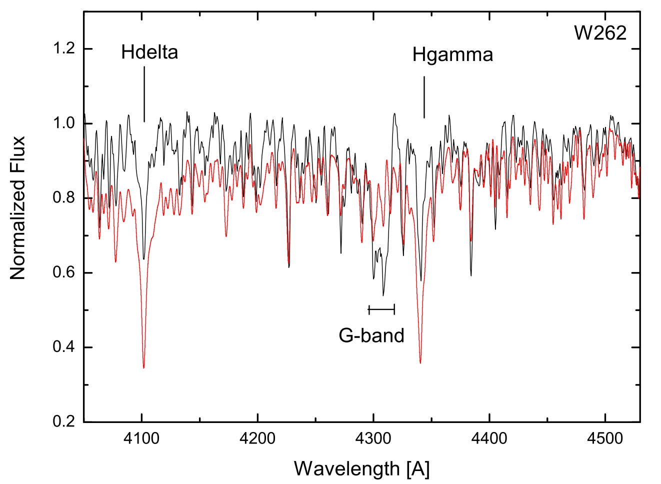

Figure 4.9: Comparison between the observed (black) and the synthetic spectrum (red) of W262 with a T_{eff} of 6500 K, log g of 4.0 and a $v \cdot \sin i$ of 100 km/s.

4.3.2 NGC 6530

NGC 6530 is an extremely young cluster embedded in the central part of the star forming region M8, the Lagoon nebula (Zwintz et al., 2006). Due to the interaction of the star cluster with the surrounding star forming region, there are a lot of stars showing emission lines.

NGC 6530 W38

Photometric analyses of NGC 6530 W38 yielded a V of 12.18 mag, a (B-V) of 0.48 mag and an (U-B) of 0.32 mag (van den Ancker et al. 1997). Chini and Neckel (1981) identified a spectral class of A0/A5 and an effective temperature of 9700 K for this star. NGC 6530 W38 is one of six pre-main sequence pulsators with δ Scuti type pulsations (Zwintz et al. 2006). Its light curve showed multi-periodicity with nine significant frequencies. The membership probability varies according to different authors. It has a membership probability of 68% according to the studies of van Altena and Jones (1972). Kharchenko et al. (2005) derived a membership of only 42% and the most recent studies belonging to Chen et al. (2007) classified the membership probability with 99%.

From the spectrum analyses an effective temperature of 7200 $\pm$ 300 K, a log g of 4.0 $\pm$ 0.5 and a $v \cdot \sin i$ of 100 $\pm$ 50 km/s could be derived. The star showed the Hγ and Hδ lines in emission (an expample is given in Fig. 4.10).

NGC 6530 W53

Chini and Neckel (1981) determined a V of 13.11 mag, a (B-V) of 0.57 mag and an (U-B) of 0.470 mag for NGC 6530 W53. They also derived a spectral class of A0 for this star. NGC 6530 W53 has a cluster membership probability of 78% according to van Altena and Jones (1972) and a probability of 99% according to Chen et al. (2007). Frequency analyses of Zwintz et al. (2006) identified five δScuti type frequencies. Therefore it has been classified as a pre-main sequence pulsator.

For NGC6530 W53 an effective temperature of 6900 $\pm$ 400 K and a surface gravity of 4.0 $\pm$ 0.5 was derived. The $v \cdot \sin i$ value seems to be very small if any, that it could not be determined from the observed spectra. Both hydrogen lines, Hδ and Hγ are in emission. Further the Fe I lines at $\lambda =$ 4254.4 Å and $\lambda =$ 4471.68 Å are in emission, which can be clearly seen within Figure 4.11. The G-band is visible at $\lambda =$ 4300 Å.

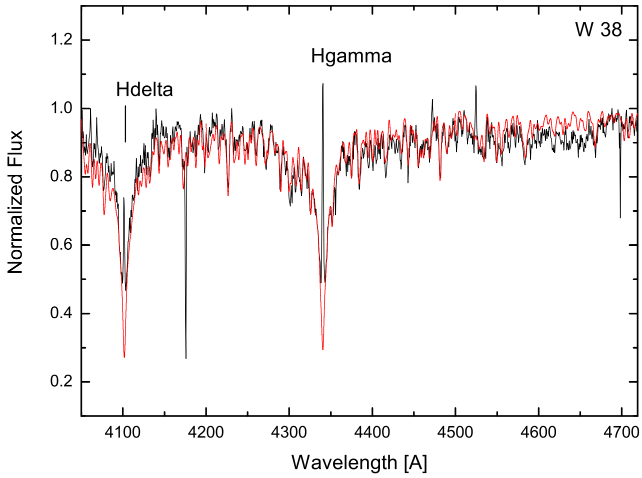

Figure 4.10: Comparison between the observed (black) and the synthetic spectrum (red) of W38 with a $T_{\rm eff}$ of 7200 K, log g of 4.0 and a $v \cdot \sin i$ of 100 km/s. The emission in Hδ and Hγ is clearly visible. The other visible absorption and emission features are reduction artifacts.

NGC 6530 W57

NGC 6530 W57 is another one of the pulsating pre-main sequence stars of NGC 6530, which showed δ Scuti like pulsations (Zwintz et al., 2006). Walker (1957) derived a V = 13.66 mag, a (B-V) = 0.49 mag and an (U-B) = 0.23 mag. Van Altena and Jones (1972) found its cluster membership to be 0%. No spectral type was available in the literature.

Model calculations yielded a temperature of 8000 ± 500 K, a log g of 4.0± 0.5 and a $v \cdot \sin i$ of 25 ± 25 km/s. The $v \cdot \sin i$ value is so small if any, that it was not detectable with these low resolution spectra. Several emission lines could be detected: the Hγ, Hδ and the Fe II line at 4303.22 Å (an example is given in Figure 4.12).

NGC 6530 W75

NGC 6530 W75 has a V of 14.171 mag, a (B-V) of 0.972 mag and an (U-B) of 0.49 mag (Sung et al 2000). It is denoted as a variable star (Zwintz et al 2006). There was no membership probability or spectral type available in the literature.

From the calculated models in this work an effective temperature $T_{\rm eff}$ of

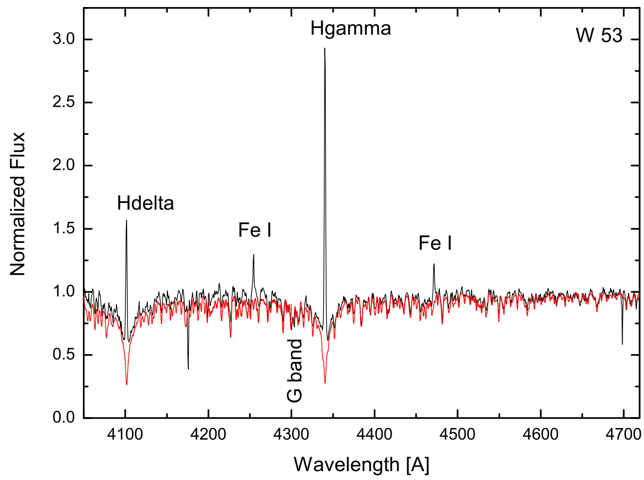

Figure 4.11: Comparison between the observed (black) and the synthetic spectrum (red) of W53 with a T_{eff} of 6900 K, log g of 4.0 and a $v \cdot \sin i$ of 0 km/s. The emission lines can clearly be identified.

6000 ± 500 K, a log g of 4.0 ± 0.5 and a $v \cdot \sin i$ of 20 ± 20 km/s could be derived. The $v \cdot \sin i$ value again is so small that it cannot be detected with these low resolution spectra. Furthermore Hγ and Hδ were in emission and also Fe I at $\lambda = 4471$ Å. The G-Band is also present (Figure 4.13).

NGC 6530 W78

According to Zwintz et al. (2006) NGC 6530 W78 has a V of 13.995 mag, and a (B-V) of 0.542 mag and according to Sung et al. (2000) it has an (U-B) of 0.298 mag. Frequency analyses performed by Zwintz et al. (2006) yielded three pulsation frequencies. No membership probabilities or references to a spectral type were found in the literature.

Our spectral analysis indicates an effective temperature of 6900 ± 300 K, a log g of 4.0 ± 0.5 and a $v \cdot \sin i$ of 50 ± 25 km/s. The spectrum shows both Balmer lines Hγ and Hδ in emission, as well as the Fe I lines at $\lambda = 4385$ Å, $\lambda = 4471$ Å, $\lambda = 4489$ Å and $\lambda = 4656{,}5$ Å and one Fe II line at $\lambda = 4114$ Å (Figure 4.14).

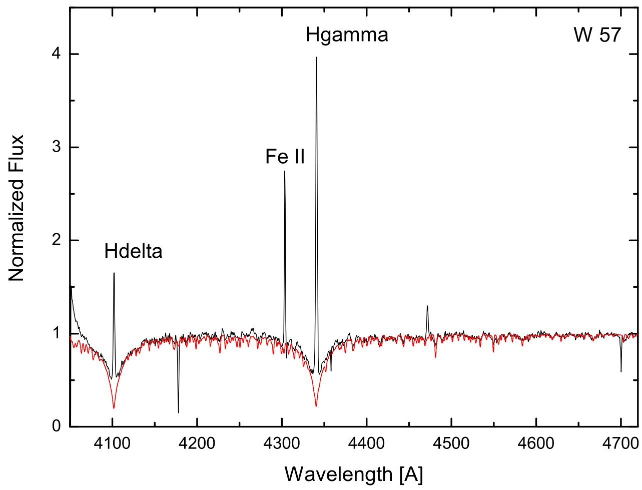

Figure 4.12: Comparison between the observed (black) and the synthetic spectrum (red) of W 57 with a T_{eff} of 8000 K, log g of 4.0 and a $v \cdot \sin i$ of 0 km/s. The emission lines are clearly visible.

NGC 6530 W94

UBV photoelectric observations of Walker (1957) and van den Ancker et al. (1997) derived V = 12.65 mag, (B-V) = 0.26 mag and (U-B) = -0.020 mag. The membership probability of W94 to NGC 6530 is reported to be 25% (van Altena et al., 1972). A multiwavelength study performed by van den Ancker et al. (1997) derived a spectral type of A0 for W94 with an effective temperature of 9700 K.

Figure 4.15 presents the spectrum for NGC 6530 W94. The G-band is clearly visible, the Hγ line is in emission. The emission in Hδ was not clearly detectable. The effective temperature was determined to be 6000 $\pm$ 300 K. The log g is 4.0 $\pm$ 0.5 and the $v \cdot \sin i$ = 100 $\pm$ 30 km/s.

NGC 6530 W114

According to the studies of Walker (1957), NGC 6530 W114 has a V of 11.98 mag, a (B-V) of 0.35 mag and an (U-B) of 0.26 mag. Only a 1D spectral classification of van den Ancker (1997) is available in the literature, which defines W114 as a B5e star. According to the observations of Chen et al. (2007) its membership probability is 98 % and according to Altena et al.

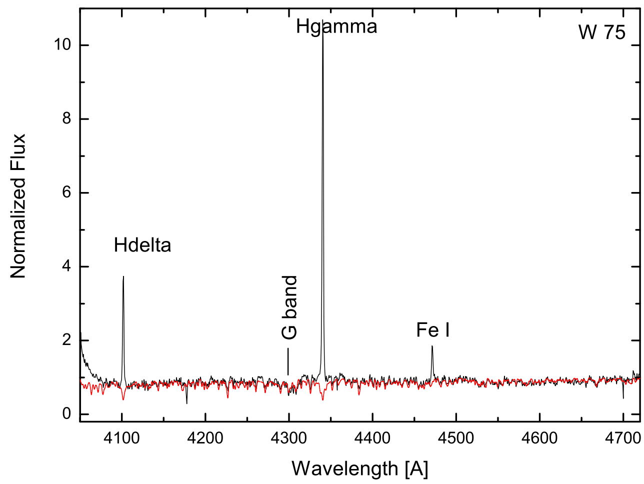

Figure 4.13: Comparison between the observed (black) and the synthetic spectrum (red) of W75 with a T_{eff} of 6000 K, log g of 4.0 and a $v \cdot \sin i$ of 20 km/s.

(1972) it is 79 %. Zwintz et al. (2007) classified W114 as a binary star from times series photometry.

The spectral analysis yields a T_{eff} of 16000 ± 500 K, a log g of 4.0 ± 0.5 and a $v \cdot \sin i$ of 50 ± 25 km/s. No lines in emission could be recognized. There are strong absorption features of He I at λ = 4120.8 Å, λ = 4387.9 Å, λ = 4471.7 Å and λ = 4713.1 Å. Additionally there is one absorption line of Mg II at λ = 4481.3 Å. The strong absorption feature at λ = 4176.2 is a reduction artifact. The asymmetry of both hydrogen lines Hδ and Hγ, could be an indicator for the binary nature of W114 . The Hγ line contains a double peak, which results possibly from a second signal that also would underline the binary nature of the star (Figure 4.17).

NGC 6530 W159

Sung et al. (2000) performed UBV CCD observations and derived for NGC 6530 W159 a V = 13.592 mag, a (B-V) = 0.435 mag and an (U-B) = 0.263 mag. It is classified as a pre-main sequence pulsator with two frequencies (Zwintz et al. 2006). In the literature there is neither a spectral type nor a membership probability available. From the spectroscopic analyses in this work an effective temperature of 7200 ± 300 K, a log g of 4.0 ± 0.5 and a

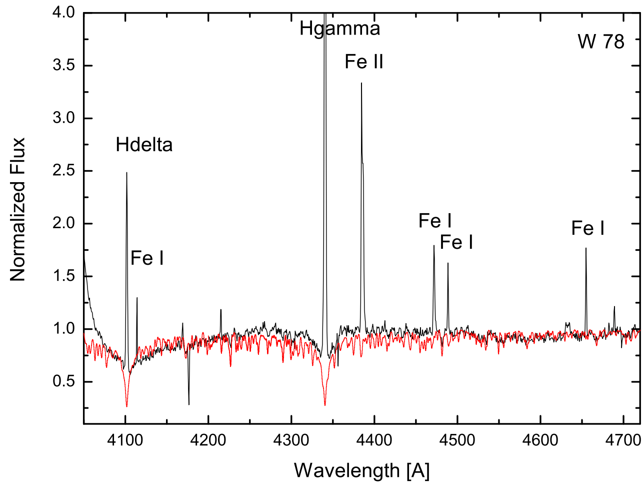

Figure 4.14: Comparison between the observed (black) and the synthetic spectrum (red) of W78 with a T_{eff} of 6900 K, log g of 4.0 and a $v \cdot \sin i$ of 50 km/s. Emission lines are clearly visible.

$v \cdot \sin i$ of 50 ± 20 km/s is derived. In Figure 4.18 emission lines are clearly visible. Hγ and Hδ were in emission and also Fe I at $\lambda = 4244$ Å and $\lambda = 4471.6$ Å. The G-band can be seen at $\lambda = 4300$ Å.

Another interesting feature is the double peak which can be seen within the Hδ line. Investigations of Hα lines performed by Vieira et al. (2003) and Reipurth et al. (1996), showed, that the line profile is changing from a single to a double peak or the other way round. Both authors tried to define four types of line profiles. Stars belonging to the first type (type I) have symmetric Hα profiles, with no or only slight influence from absorption features (Reipurth et al., 1996). The second and the third type only differ in the strength of the two double peaks. They made a difference, if the second peak is more than (type II) or less than (type III) half the strength of the first one. The last type (type IV) showed P Cygni line profiles, that is, the absorption has a sufficient velocity to be present beyond the wing of the underlying emission line, and no secondary peak is visible (Reipurth et al., 1996). In the spectrum of NGC 6530 W159 such a double peak of type III is visible within the Hδ line (Figure 4.19). That means, that the first peak exceeds half the strength of the primary peak. The origin of these variations of the hydrogen lines is discussed by various authors. Vieira et al (2003) tried to explain these variations with interactions with circumstellar mate-

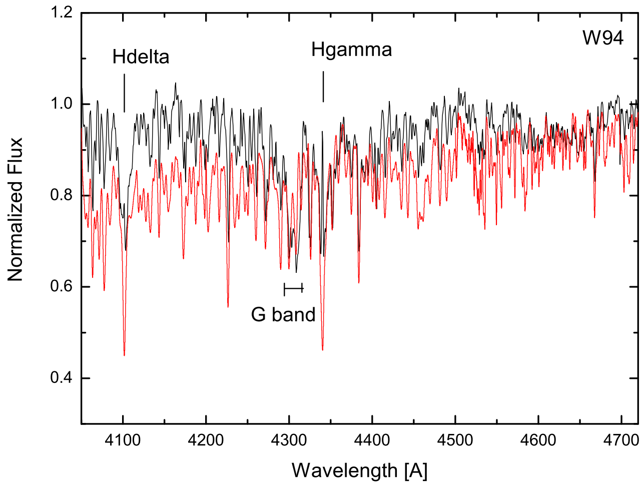

Figure 4.15: Comparison between the observed (black) and the synthetic spectrum (red) of W94 with a T_{eff} of 6000 K, log g of 4.0 and a $v \cdot \sin i$ of 100 km/s. Hγ is in emission. Hδ could not be identified clearly to be in emission.

rial of stellar winds caused by planetesimal bodies orbiting around the star. Another explanation are possible magnetic fields around Herbig Ae/Be stars generating stellar winds (Reipurth et al, 2006). Also different velocity gradients caused by stellar winds were taken into account. In the case of W159, the interaction with circumstellar material seems to be the most probable, because there are a lot of emission lines clearly visible within the spectrum and the star is located in the remnants of his birth cloud.

NGC 6530 W161

Sung et al. (2000) derived a V of 13.753 mag, a (B-V) of 0.578 mag and an (U-B) of 0.139 mag. There is neither a spectral type, nor a membership probability available in the literature.

Spectroscopic analyses yield a T_{eff} of 26 000 $\pm$ 6000 K, a log g = 4.0 $\pm$ 0.5 and a $v \cdot \sin i = 150 \pm 50$ km/s. The spectrum shows no emission lines. Both hydrogen lines Hδ and Hγ are very strong. Additionally there are strong absorption lines of He I at λ = 4120.8 Å, λ = 4143.7 Å, λ = 4387.9 Å, λ = 4471.5 Å and λ = 4713.1 Å denoting the hot nature of the star. Further there is a relatively strong absorption feature of Mg II at λ = 4481.3 Å. The depression within the spectrum at λ = 4310 Å could not be dispersed to

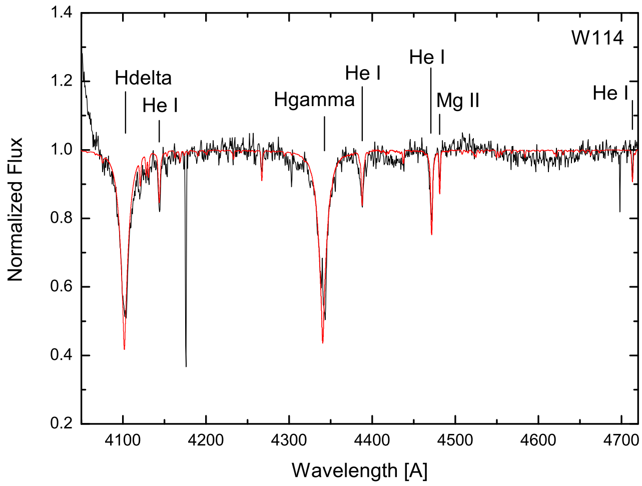

Figure 4.16: Comparison between the observed (black) and the synthetic spectrum (red) of W114 with a T_{eff} of 16000 K, log g of 4.0 and a $v \cdot \sin i$ of 50 km/s. Many He I lines are clearly visible within the spectrum, denoting the hot temperature of the star. The strong absorption feature at $\lambda = 4176.2$ is a reduction artifact.

single elements and might be a reduction artifact.

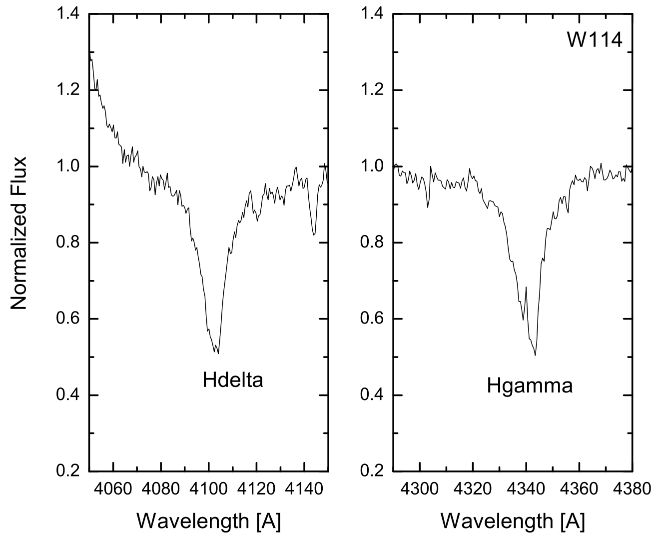

Figure 4.17: Hδ and Hγ lines for W114. Left: Hδ line with asymmetric wings; right: Hγ line with a double peak, that might be of a second star and underlines the possible binary nature of W114.

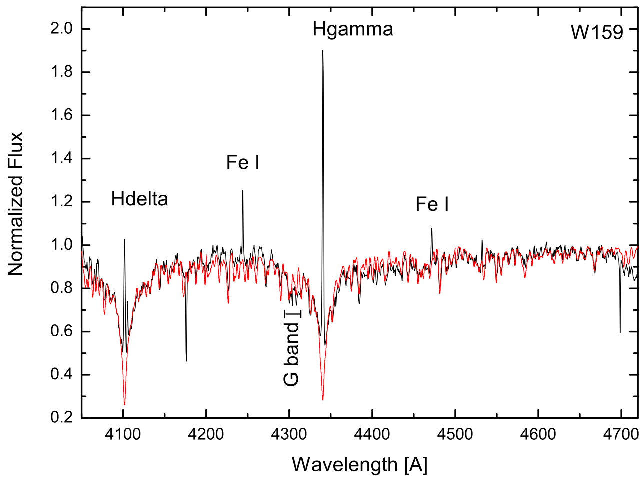

Figure 4.18: Comparison between the observed (black) and the synthetic spectrum (red) of W159 with a T_{eff} of 7200 K, log g of 4.0 and a $v \cdot \sin i$ of 80 km/s. Both hydrogen emission lines Hδ and Hγ are clearly visible. Two Fe I lines are also in emission.

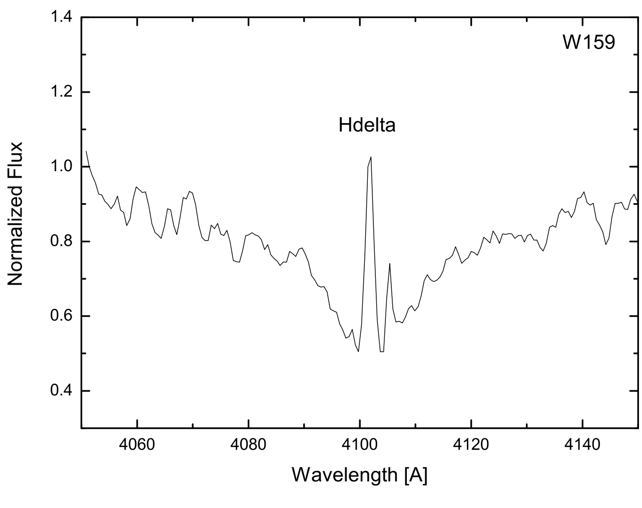

Figure 4.19: The Hδ line of W159 contains a double peak of type III. This feature is explained as a result of interaction of the star with the surrounding circumstellar matter.

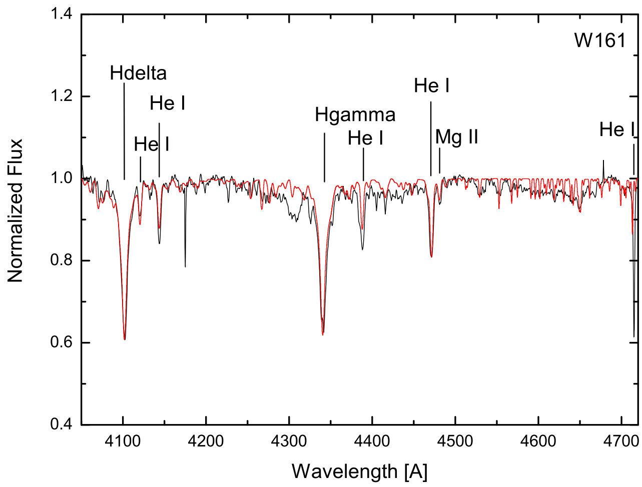

Figure 4.20: Comparison between the observed (black) and the synthetic spectrum (red) of W161 with a T_{eff} of 26000 K, log g of 4.0 and a $v \cdot \sin i$ of 150 km/s. Both hydrogen lines Hδ and Hγ are in absorption and there are a lot of He I lines visible within the spectrum.

4.3.3 NGC 6611

NGC 6611 is a young cluster that is located in the constellation of Serpens embedded in the Sagittarius spiral arm and is probably associated with the emission nebula M 16, the Eagle Nebula, (Belikov et al. 1999). It is a very peculiar cluster embedded in a lot of dust. Some of the observed stars showed emission lines.

NGC 6611 W41 #119

UBV CCD observations derived V = 14.15 mag, (B-V) = 0.85 mag and (U-B) = 0.27 mag. (Hillenbrand et al., 1993). There are also some JHK observations available from Hillenbrand et al. (1993). They derived values for J = 12.28 mag, H = 12.01 mag, K = 11.96 mag, (J-H) = 0.27 mag, (H-K) = 0.05 mag and (J-K) = 0.32 mag. According to Tucholke et al. (1986) W41 is not a member of NGC 6611. Belikov et al. (1999) designated its membership probability with 30%. There is no spectral type available from NGC 6611 W41 in the literature.

The effective temperature of this star is derived to be 6000 ± 200 K, a log g = 4.0 ± 0.5 and a $v \cdot \sin i$ = 100 ± 20 km/s. There are no emission lines visible, but the G-band at λ = 4300 Å.

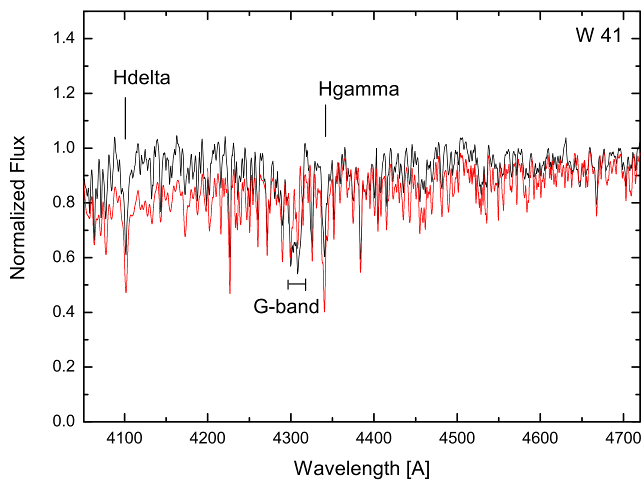

Figure 4.21: Comparison between the observed (black) and the synthetic spectrum (red) of W41 with a $T_{\rm eff}$ of 6000 K, log g of 4.0 and a $v \cdot \sin i$ of 50 km/s.

NGC 6611 W43 #148

NGC 6611 W43 has a V of 14.47 mag, a (B-V) of 0.86 mag and an (U-B) of 0.43 mag (Hillenbrand et al. 1993). There are also some JHK observations available (Hillenbrand et al., 1993): J = 12.52 mag, H = 12.37 mag, K = 12.17 mag, (J-H) = 0.15 mag, (H-K) = 0.20 mag and (J-K) = 0.35 mag. Belikov et al. (1999) reported the membership probability to be 0%, so this star seems not to be a cluster member. No spectral type or pulsation frequencies could be derived from literature.

Figure 4.22 shows the spectrum of NGC 6611 W43. There are no emission lines visible, but the G-band. The effective temperature was obtained with 6000 ± 300 K, a log g = 4.0 ± 0.5 and a $v \cdot \sin i$ = 80 ± 20 km/s.

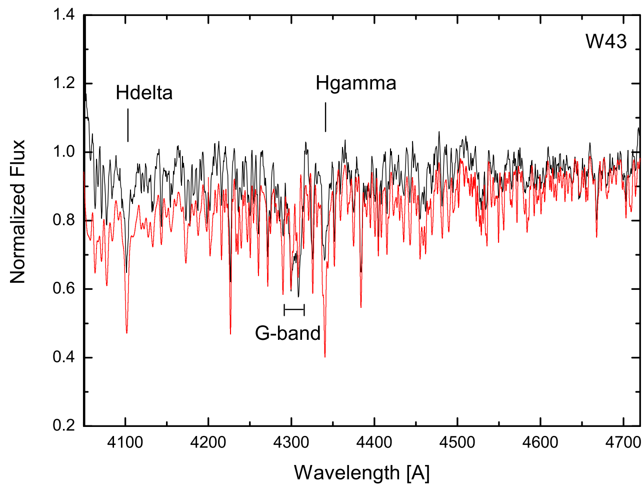

Figure 4.22: Comparison between the observed (black) and the synthetic spectrum (red) of W43 with a $T_{\rm eff}$ of 6000 K, log g of 4.0 and a $v \cdot \sin i$ of 50 km/s.

NGC 6611 W110 #88

NGC 6611 W110 has a V = 14.50 mag, a (B-V) = 0.76 mag and an (U-B) = 0.47 mag according to Hillenbrand et al. (1993). Guarcello et al. (2007) derived JHK values: J = 12.771 mag, H = 12.515 mag, K = 12.395 mag, (J-H) = 0.256 mag, (H-K) = 0.12 mag and (J-K) = 0.376 mag. Its membership probability is reported to be 70% derived from spatial and proper motions distributions (Belikov et al. 1999).

This star shows one emission line at $\lambda = 4701$ Å of Fe I. The emission of the Hδ line was too small to be detected. From the spectroscopic analyses $T_{\rm eff} = 6000 \pm 500$ K, a log g = 4.0 ± 0.5 and a $v \cdot \sin i = 50 \pm 20$ km/s were derived.

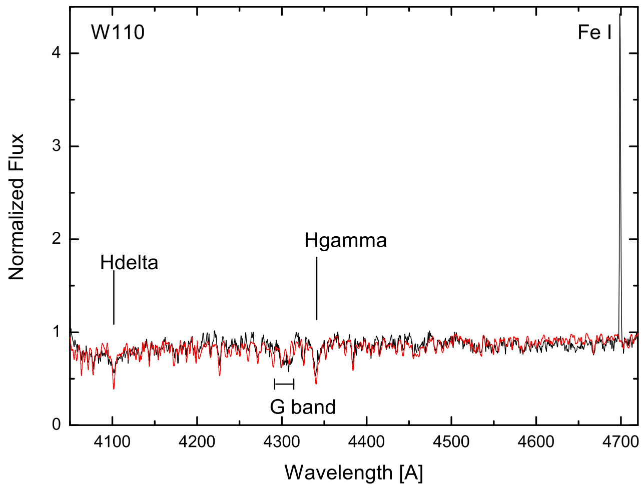

Figure 4.23: Comparison between the observed (black) and the synthetic spectrum (red) of W110 with a $T_{\rm eff}$ of 6000 K, log g of 4.0 and a $v \cdot \sin i$ of 50 km/s. One clear emission line of Fe I is visible.

NGC 6611 W221 #71

Hillenbrand et al. (1993) derived UBV values from CCD observations of V = 14.55 mag, (B-V) = 1.02 mag, (U-B) = 0.62 mag Also JHK observations were performed in the same study. They obtained the following values: J = 11.33 mag, H = 11.12 mag, K = 10.78 mag, (J-H) = 0.21 mag, (H-K) = 0.34 mag and (J-K) = 0.55 mag. The membership probability of W 221 was determined to be 89% (Belikov et al., 1999). Hillenbrand et al. (1993) obtained a spectral type of B8 Ve.

NGC 6611 W221 shows no emission lines. Its spectrum contains a lot of He I and He II lines. He I is in absorption at $\lambda = 4143.76$ Å, $\lambda = 4387.9$ Å and $\lambda = 4471.5$ Å. He II is in absorption at $\lambda = 4199.8$ Å, $\lambda = 4541.6$ Å and $\lambda = 4685.7$ Å. This indicates that NGC 6611 W221 is a hot star. Furthermore there is a very significant structure visible within the spectrum at $\lambda = 4430$ Å, a diffuse interstellar band (DIB). The first appearance of this band in a heavily reddened giant B star was misidentified as Hγ (Merrill 1936; Code 1958). Further observations derived by other authors classified it as one of meanwhile 39 diffuse absorption features in the wavelength range between 4400 Å and 6850 Å (Herbig 1975). It is of interstellar origin and appears in connection with highly reddened O or B type stars surrounded by an high amount of dust (Herbig 1962). The band at $\lambda = 4430$ Å is broad and diffuse with a complex profile. Its great width makes it difficult to associate the line with atomic absorption and no definite chemical identification of this line has been found (Beals et al. 1938). According to Herbig (1962) molecular hydrogen or helium must be involved for the formation of this band. The process, leading to that absorption feature seems to be effective only for hot stars lying in a dusty region. Therefore it seems to be probably more a circumstellar phenomenon than an interstellar one.

The effective temperature is derived to be 35 000 ± 2000 K, the log g = 4.0 ± 0.5 and the $v \cdot \sin i = 180 \pm 20$ km/s.

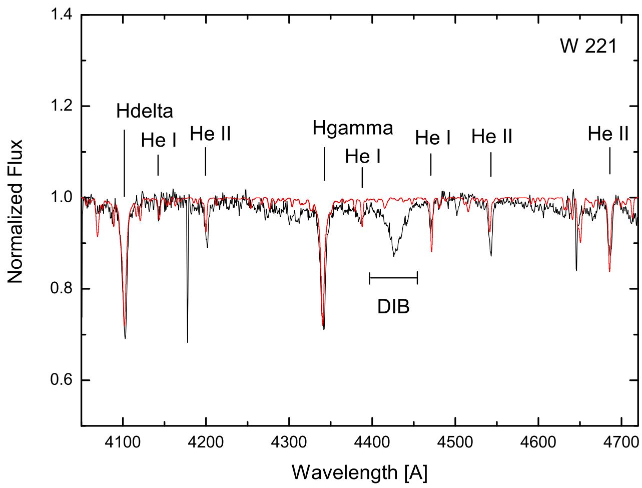

Figure 4.24: Comparison between the observed (black) and the synthetic spectrum (red) of W221 with a T_{eff} of 35000 K, log g of 4.0 and a $v \cdot \sin i$ of 100 km/s. He I and He II lines are clearly visible, denoting the hot nature of the star. A diffuse interstellar band (DIB) is visible, which appears in hot stars surrounded by circumstellar dust.

NGC 6611 W260 #7

According to UBV CCD observations of Hillenbrand et al. (1993) NGC 6611 W260 has a V = 14.38 mag, (B-V) = 0.76 mag and an (U-B) = 0.46 mag. Its membership probability is 20% (Belikov et al. 1999). There was no spectral type available in the literature of this star.

NGC 6611 W260 shows both hydrogen lines, Hγ and Hδ, in emission and also the Fe I lines at λ = 4273.4 Å, λ = 4382.6 Å, λ = 4388.59 Å and λ = 4685 Å are in emission.The effective temperature was determined to be 6900 $\pm$ 300 K, a log g = 4.0 $\pm$ 0.5 and a $v \cdot \sin i$ = 80 $\pm$ 30 km/s.

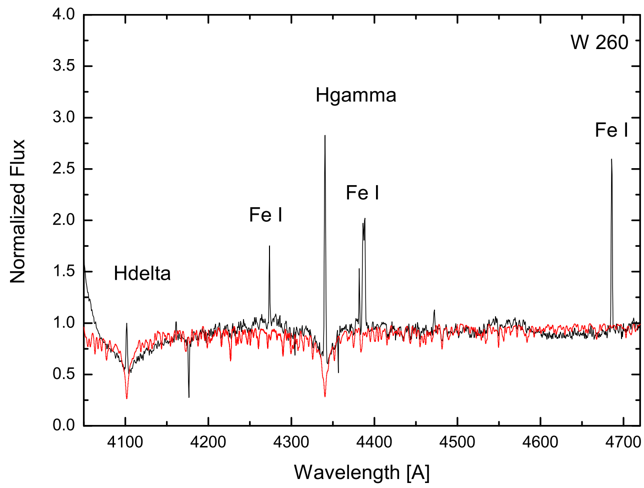

Figure 4.25: Comparison between the observed (black) and the synthetic spectrum (red) of W260 $T_{\rm eff}$ of 6900 K, log g of 4.0 and a $v \cdot \sin i$ of 50 km/s. Emission lines are clearly visible within the spectrum.

NGC 6611 W292 #82

V = 14.09 mag, (B-V) = 0.78 mag and (U-B) = 0.41 mag are reported for NGC 6611 W292 (Hillenbrand et al. 1993). JHK observations were performed by Hillenbrand et al. (1993) and Guarcello et al. (2007). The values are as following: J = 12.36 mag, H = 12.32 mag, K = 12.14 mag, (J-H) = 0.04 mag, (H-K) = 0.18 mag and (J-K) = 0.22 mag. Contradicting membership probabilities were derived from proper motion studies from Tucholke et al. (1986) as 29% and from Belikov et al. (1999) as 84%. No spectral type was available in the literature.

The effective temperature was derived to be 6000 ± 500 K, a log g = 4.0 ± 0.5 and a $v \cdot \sin i$ = 25 ± 25 km/s was derived. There are three emission lines present of Fe I at λ = 4085.1 Å, λ = 4158.8 Å and λ = 4239.4 Å. Both hydrogen lines, Hδ and Hγ are in absorption.

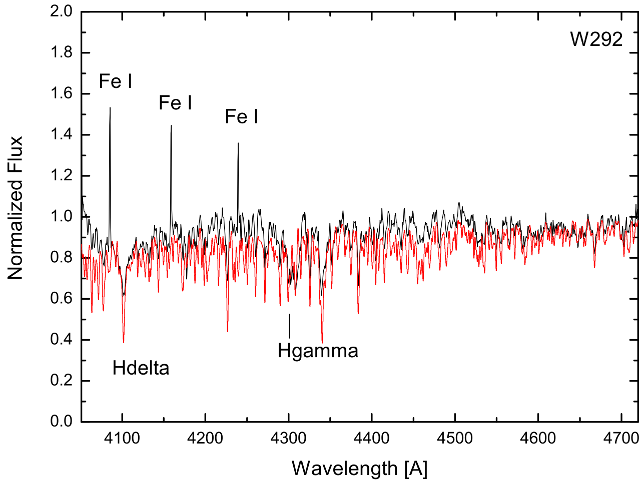

Figure 4.26: Comparison between the observed (black) and the synthetic spectrum (red) of W292 with a T_{eff} of 6000 K, log g of 4.0 and a $v \cdot \sin i$ of 50 km/s. Emission lines of Fe I are clearly visible within the spectrum.

Chapter 5

Conclusion

5.1 Pulsating pre-main sequence stars in NGC 6611

The first aim of this work was the search for pulsating pre-main sequence stars within the young open cluster NGC 6611. CCD photometry during an observational period of 14 nights was performed and the light curves were analyzed with the Fourier based program Period 04. Among the 186 selected stars, four stars showed periodic behavior. Two stars, #7 (NGC 6611 W260) and #71 (NGC 6611 W221) were monoperiodic and two, #82 (NGC 6611 W292) and #180 (NGC 6611 W374) showed a multiperiodic behavior. The frequencies and periods are listed in Table 5.1.

star	Webda	freq. [c/d]	period	amp. [mag]
7	260	25.148	57.3 minutes	0.003
71	221	9.316	2.58 hours	0.010
82	292	29.876	48.2 minutes	0.002
		25.697	56.04 minutes	0.002
		23.189	1.03 hours	0.001
180	374	7.739	3.1 hours	0.011
		6.436	3.73 hours	0.006
		13.335	1.80 hours	0.003
		12.875	1.86 hours	0.002
		8.526	2.81 hours	0.01
		5.158	4.65 hours	0.002

Table 5.1: Identified pulsation frequencies and periods of the four pulsating stars in NGC 6611.

The other remaining 182 stars were either inconclusive or showed no periodic behavior. With the detection of those four stars, the total number of already classified pulsating pre-main sequence stars is raised by four. The position of all 186 observed stars in the observational HRD can be seen in Figure 5.1. The magnitudes and colors for all stars are taken from WEBDA. The four pulsating variable pre-main sequence stars are the blue ones.

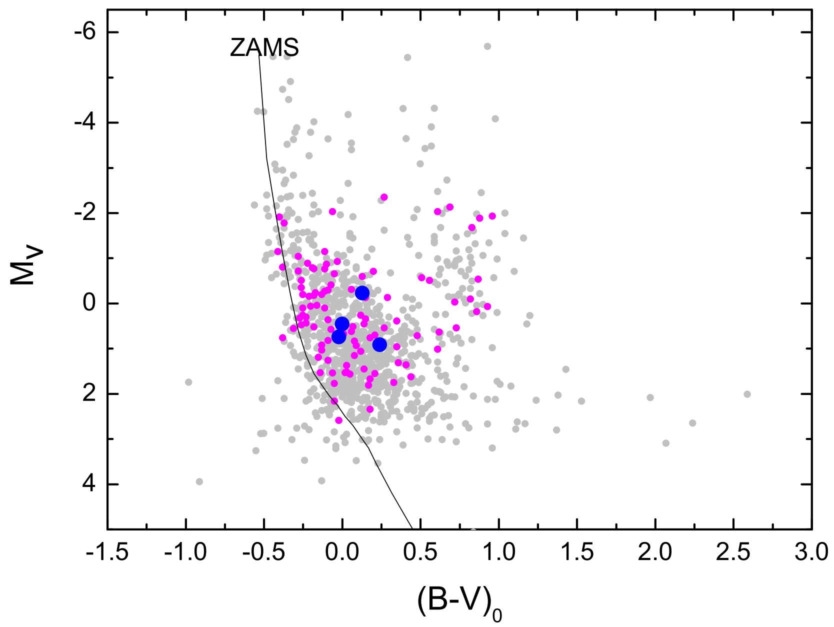

Figure 5.1: Observational HRD of NGC 6611. Colors and magnitudes of all stars are taken from WEBDA. The gray stars are all available stars taken from the WEBDA database. The pink stars are the 186 observed stars and the blue stars are the four newly discovered pulsating pre-main sequence stars. The solid line represents the ZAMS (Schmidt-Kaler 1965)

5.2 Fundamental parameters for stars in NGC 6530, NGC 6383 and NGC 6611

For the second part of this work, a selection of previously identified pulsating pre-main sequence stars out of the clusters NGC 6611, NGC 6383 and NGC 6530 were taken and spectroscopically analyzed to derive fundamental properties, such as effective temperature, surface gravity and $v \cdot \sin i$. Only for a few stars spectral types were available in the literature. Each spectrum was compared with Kurucz models. Several stars showed typical emission lines for Herbig Ae/Be stars.

5.2.1 NGC 6383

Three pulsating pre-main sequence stars were selected from NGC 6383: W54, W55 and W262. All three stars are located near the bright spectroscopic binary HD 159176, located in the central part of the cluster, as it can be seen in Figure 5.2. Only for the star W54 a spectral type was available in the literature by Thé et al. (1985). The authors derived a spectral type F0Ve, but they could not clearly distinguish between the effective temperatures of 6500 K and 7500 K. From our analyses an effective temperature of 6500 K can be confirmed. There was no good fit with the synthetic spectrum of 7500 K.

For W55 an effective temperature of 7345 K was determined from Johnson V and (B-V) values according to Kenyon et al. (1995). According to our spectral analysis W55 has an effective temperature of 6900 K. The $v \cdot \sin i$ value for this star was hardly detectable and is 25 ± 25, because of the low resolution of the spectra.

W262 has an effective temperature of 6500 K in our analysis. All three stars showed no emission lines. A summary of the derived fundamental parameters of all three stars is given in Table 5.2.

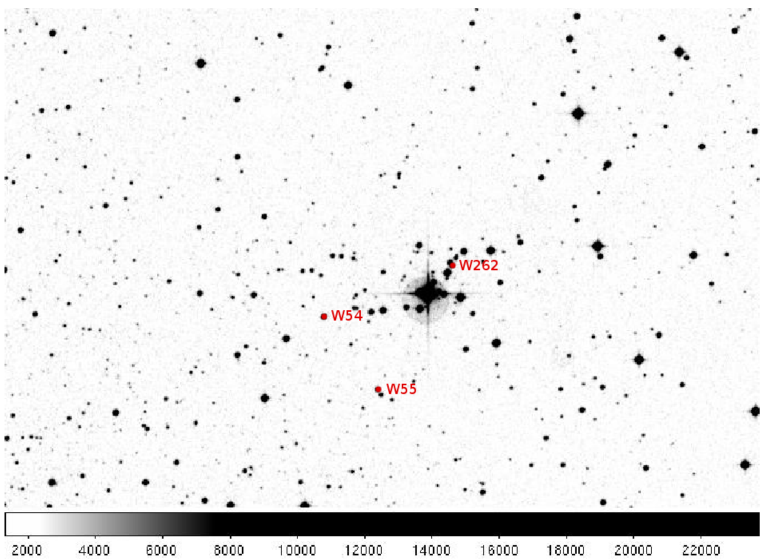

Figure 5.2: DS9 image for NGC 6383 showing the bright central binary HD 159176 and the three observed stars.

Object ID	T_{eff}	log g	$v \cdot \sin i$	emission lines
NGC 6383 W54	6500 ± 300 K	4.0 ± 0.5	80 ± 30 km/s	-
NGC 6383 W55	6900 ± 300 K	4.0 ± 0.5	25 ± 25 km/s	-
NGC 6383 W262	6500 ± 300 K	4.0 ± 0.5	25 ± 25 km/s	-

Table 5.2: Fundamental parameters; the W numbers correspond to the WEBDA numbering system.

5.2.2 NGC 6530

In total spectra of nine stars were obtained and analyzed. Due to the interaction of NGC 6530 with the surrounding star forming region, nearly all stars showed emission lines within their spectra. Emission lines are present for Hδ, Hγ, Fe I and Fe II. A summary of all emission lines and fundamental parameters is given in Table 5.3. The most important highlights are listed in the following.

Only for three stars a spectral type was available in the literature. Chini and Neckel (1981) derived a spectral class of A0/A5 and an effective temperature of 9700 K for W38 and a spectral class of A0 for W53. The value for the effective temperature of W38 could not be confirmed out of this study. In our analysis it showed an effective temperature of 7200 K and both hydrogen Balmer lines Hδ and Hγ in emission.

Van den Ancker et al. (1997) derived a spectral class of A0 for W94 out of multiwavelength studies and an effective temperature of 9700 K. Concerning our spectral studies, in the spectrum (Figure 4.15) the G-band is clearly visible which only appears in cooler stars. The temperature of W94 is classified with 6000 ± 300 K.

W114 is a really hot star that shows a lot of He I lines. Van den Ancker (1997) derived a spectral type of B5e. This star is disputed to be a binary. One evidence for the binary nature of this star could be the visible asymmetry in both hydrogen lines Hδ and Hγ. For details see Figure 4.17 in the previous chapter. There is also a double peak visible in the Hγ line which underlines the possible binary nature of the star, too.

Another interesting feature was observed within the spectrum of W159. Investigations of Hα lines performed by Vieira et al. (2003) and Reipurth et al. (1996), showed a changing line profile. They classified four groups according to the four different types of the line appearance. Such a line profile is visible within the Hδ line of W159 (see Figure 4.19 in the previous chapter). The appearing line profile belongs to their group III. That means that the second peak is half the strength of the first one. The reason for this kind of double peak is explained by the interaction of the star with its circumstellar surrounding.

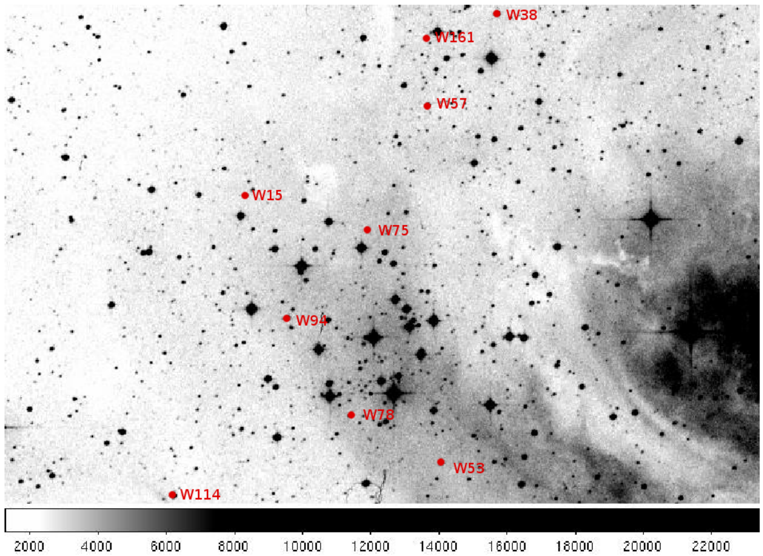

Figure 5.3: DS9 image of NGC 6530 with the observed stars.

5.2.3 NGC 6611

In total spectra of six stars were obtained and analyzed. All derived fundamental parameters are listed in Table 5.4. The most interesting features are discussed in the following.

Only for one of the observed stars a spectral type was available in the literature. Hillenbrand et al. (1993) derived a spectral type of B8Ve for W221. Also in the present analysis it is a really hot star with an effective temperature of 35000 K. Its spectrum contains He I and He II lines. A problem that occurred in modeling this star, was to fit the He I and He II lines at the same time. To get a better fit for the He II lines a non LTE model would be necessary, but such models are currently only under development. Another interesting feature is visible at the wavelength λ = 4430 Å. It is known as a diffuse interstellar band, that occurs in highly reddened B stars surrounded by circumstellar dust. It is another hint that W221 is a hot star embedded in a dusty region.

Among the observed stars, there were three stars showing emission lines: W110, W260 and W292. The other three stars showed no emission lines. Three of the four pulsating pre-main sequence stars found in the first part (W260, W221 and W292) were analyzed spectroscopically. Except star W221, the other two showed emission lines.

Object ID	$T_{\rm eff}$	log g	$v \cdot \sin i$	emission lines
NGC 6530 W38	7200 ± 300 K	4.0 ± 0.5	100 ± 50 km/s	Hδ, Hγ
NGC 6530 W53	6900 ± 400 K	4.0 ± 0.5	25 ± 25 km/s	Hδ, Hγ, Fe I
NGC 6530 W57	8000 ± 500 K	4.0 ± 0.5	25 ± 25 km/s	Hδ, Hγ, Fe II
NGC 6530 W75	6000 ± 500 K	4.0 ± 0.5	20 ± 20 km/s	Hδ, Hγ, Fe I
NGC 6530 W78	6900 ± 300 K	4.0 ± 0.5	50 ± 25 km/s	Hδ, Hγ, Fe I, Fe II
NGC 6530 W94	6000 ± 300 K	4.0 ± 0.5	100 ± 30 km/s	Hγ
NGC 6530 W114	16000 ± 500 K	4.0 ± 0.5	50 ± 25 km/s	-
NGC 6530 W159	7200 ± 300 K	4.0 ± 0.5	50 ± 20 km/s	Hδ, Hγ, Fe I
NGC 6530 W161	26000 ± 6000 K	4.0 ± 0.5	150 ± 50 km/s	-

Table 5.3: Fundamental parameters; the W numbers correspond to the WEBDA numbering system.

Object ID	$T_{\rm eff}$	log g	$v \cdot \sin i$	emission lines
NGC 6611 W41	6000 ± 200 K	4.0 ± 0.5	100 ± 20 km/s	-
NGC 6611 W43	6000 ± 300 K	4.0 ± 0.5	80 ± 20 km/s	-
NGC 6611 W110	6000 ± 500 K	4.0 ± 0.5	50 ± 20 km/s	Fe I
NGC 6611 W221	35000 ± 2000 K	4.0 ± 0.5	180 ± 20 km/s	-
NGC 6611 W260	6900 ± 300 K	4.0 ± 0.5	80 ± 30 km/s	Hδ, Hγ, Fe I
NGC 6611 W292	6000 ± 500 K	4.0 ± 0.5	25 ± 25 km/s	Fe I

Table 5.4: Fundamental parameters; the W numbers correspond to the WEBDA numbering system.

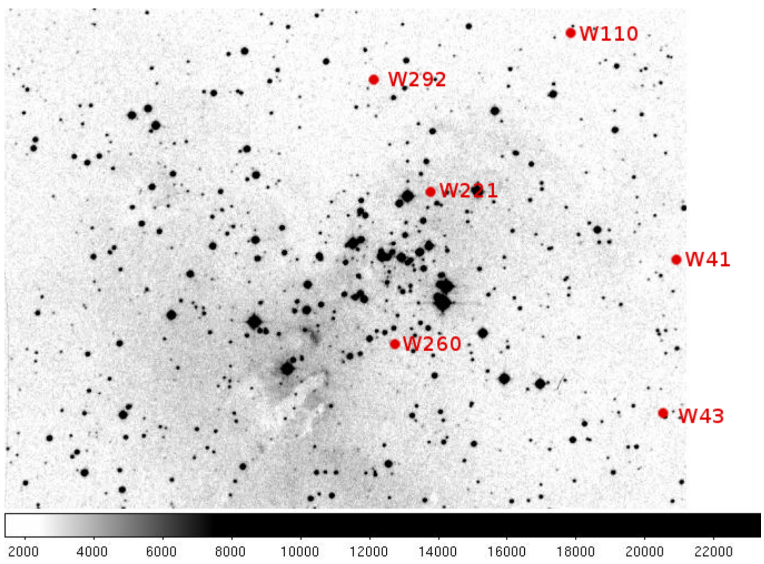

Figure 5.4: DS9 image of NGC 6611 with all observed stars.

Chapter 6

APPENDIX

Night	Image	Classification	Exp. time	Filter
1	1-10	Bias	-	-
1	11-20	Flat	110	B
1	21-30	Flat	60	V
1	31-147	NGC 6611	100	B
1	-	NGC 6611	60	V
2	-	-	-	-
3	1-10	Bias	-	-
3	11-20	Flat	110	B
3	21-31	Flat	60	V
3	32-110	NGC 6611	180	B
3	-	NGC 6611	140	V
4	1-10	Bias	-	-
4	11-20	Flat	110	B
4	21-30	Flat	60	V
4	31-32	Focus	10	-
4	33-127	NGC 6611	180	B
4	-	NGC 6611	140	V
5	1-10	Bias	-	-
5	11-20	Flat	110	B
5	21-30	Flat	60	V
5	33-x	NGC 6611	180	B
5	-	NGC 6611	140	V
6	1-10	Bias	-	-
6	11-20	Flat	110	B
6	21-30	Flat	60	V
7	1-10	Bias	-	-
7	11-20	Flat	110	B
7	21-30	Flat	60	V
7	31	Focus	-	-
7	32-134	NGC 6611	180	B
7	-	NGC 6611	140	V
8	1-10	Bias	-	-
8	11-20	Flat	110	B
8	21-30	Flat	60	V
8	31	Focus	-	-
8	32-131	NGC 6611	180	B
8	-	NGC 6611	100	V
9	1-10	Bias	-	-
9	11-20	Flat	110	B
9	21-30	Flat	60	V
9	31	Focus	-	-
9	32-133	NGC 6611	180	B
9	-	NGC 6611	140	V
10	1-10	Bias	-	-
10	11-20	Flat	110	B
10	21-30	Flat	60	V
10	31	Focus	-	-
10	32-131	NGC 6611	180	B
10	-	NGC 6611	140	V
11	1-10	Bias	-	-
11	11-20	Flat	110	B
11	21-30	Flat	60	V
11	31-33	Focus	-	-
11	34-133	NGC 6611	180	B
11	-	NGC 6611	140	V
13	1-10	Bias	-	-
13	11-20	Flat	110	B
13	21-30	Flat	60	V
13	31	Focus	-	-
13	32-131	NGC 6611	180	B
13	-	NGC 6611	120	V
14	1-10	Bias	-	-
14	11-20	Flat	110	B
14	21-30	Flat	60	V
14	31	Focus	-	-
14	32-129	NGC 6611	180	B
14	-	NGC 6611	110	V

Table 6.1: Observing log

star	Webda	x px	y px	V [mag]	B-V [mag]	U-B [mag]
1	313	493	1307	12.92	0.5	-0.07
2	299	531	1297	14.46	0.69	0.53
3	289	567	1240	12.6	0.5	-0.21
4	285	595	1211	15.16	0.81	0.74
5	276	625	1216	13.74	0.67	-0.04
6	262	659	1200	13.96	0.51	0.06
7	260	664	1263	14.38	0.76	0.46
8	240	733	1287	14.56	0.65	0.27
9	237	740	1228	15.17	0.64	0.4
10	232	762	1180	14.34	0.99	0.37
11	218	790	1200	13.61	1.5	1.23
12	211	815	1381	12.98	0.73	0.29
15	203	837	1518	14.19	0.47	0.63
18	238	730	1533	13.37	0.67	0.42
19	174	965	1640	13.04	0.91	0.27
20	194	849	1634	13.9	0.53	0.12
21	265	638	1717	11.86	0.41	0.26
23	291	552	1752	16,23	0,76	
30	169	968	1960	14.9	0.69	0.45
34	415	54	1783	15.26	1.22	0.69
40	1685	276	1321	15.01	0.81	1.34
42	388	172	1213	13.7	0.58	-0.02
43	396	149	1210	14.03	1.13	0.71
45	395	151	1104	15	1.19	0.42
46	366	284	1137	14.27	1.4	1.21
48	336	382	1109	13.29	0.52	-0.2
49	349	331	1034	11.61	1.39	1.04
50	323	471	1071	13.48	0.57	-0.02
51	273	634	1025	14.21	0.71	0.27
52	252	693	1060	13.9	0.9	0.31
53	227	774	972	12.85	0.59	-0.26
54	199	863	905	14.79	0.86	0.49
55	171	986	974	14.31	0.79	0.34
59	140	1140	1125	14.7	0.9	0.33
61	231	772	791	12.71	0.75	-0.26
62	251	703	845	13.34	0.69	-0.16
63	266	658	877	14.35	1.26	0.71
64	267	654	909	13.13	0.52	-0.22
65	322	476	949	13.68	0.62	0.09
66	297	551	770	12.88	0.67	-0.21
67	306	533	753	12.77	0.68	-0.22
68	305	535	713	13.51	1.07	-0.03
70	259	681	724	11.61	0.72	-0.33
71	221	802	684	14.55	1.02	0.62
72	213	823	724	14,18	1,51	-
73	202	861	684	14.4	0.96	0.4
74	228	784	565	13.51	0.93	-0.1
76	222	807	450	13.07	1.29	-0.04
77	364	301	318	13.44	0.53	0.01
79	417	91	144	11.96	1.61	1.78
80	340	402	184	12.75	0.56	0.38
82	292	582	255	14.09	0.78	0.41
84	151	1103	213	14.65	1.39	0.14
85	117	1267	308	11.75	1.66	1.65
89	161	1045	372	11.29	1.05	-0.25
90	144	1126	533	14	0.69	0.51
91	137	1184	575	13.71	1.71	2.31
92	128	1223	647	15.09	0.92	0.39

Table 6.2: Stars in NGC 6611 addressed in this work for which UBV values were available in the literature. Values are taken from WEBDA.

star	Webda	x px	y px	V [mag]	B-V [mag]	U-B [mag]
93	127	1224	670	15.45	0.95	-0.07
94	138	1179	712	14.83	0.63	0.41
97	79	1502	445	12.49	0.67	0.37
99	80	1509	201	13.82	1.64	-0.26
107	36	1765	742	13.4	0.61	0.34
108	26	1838	553	13.46	0.6	0.29
112	90	1435	825	11.73	0.38	-0.22
114	101	1363	843	15.31	0.96	0.3
115	89	1442	873	15.41	0.73	0.36
116	82	1480	871	14.95	1.14	0.57
119	41	1736	941	14.15	0.85	0.27
120	25	1832	937	12.93	0.98	-0.13
127	105	1325	1074	15.98	0.96	-
132	53	1664	1209	15.8	0.73	0.25
135	38	1738	1277	14.57	0.87	0.67
137	30	1804	1362	15.18	0.72	0.65
138	33	1796	1385	15.2	0.83	0.43
148	43	1693	1538	14.47	0.86	0.43
151	31	1800	1502	14.4	0.4	0.49
153	18	1871	1638	14.16	0.6	0.42
154	66	1583	1652	14.26	0.84	0.53
156	95	1386	1565	13.54	1.6	1.8
157	103	1341	1626	12.49	0.37	0.14
162	77	1495	1750	14.09	0.92	0.37
166	112	1251	1896	13.94	0.55	0.1
167	35	1756	1787	14.11	0.52	0.4
168	39	1721	1859	15.17	0.8	0.95
169	625	1872	1890	14.07	0.55	0.43
170	50	1658	1978	14.67	0.65	0.59
171	64	1585	1952	13.74	0.53	0.42
172	74	1538	1925	15.19	0.99	0.38
173	188	945	49	13.13	1.34	-0.03
174	255	707	180	13.1	1.65	1.91
175	256	701	286	14.18	1.05	0.58
176	269	658	321	13.98	0.93	-0.04
177	406	135	616	11.71	1.74	1.94
178	402	132	864	11.51	1.47	1.44
179	400	140	934	12.87	0.6	0.24
180	374	234	818	13.41	0.91	0.82
181	371	243	912	13.44	0.65	-0.07
182	433	29	154	14.6	1.13	0.12
184	327	423	1838	13.33	0.84	0.45
185	345	342	1849	13.23	0.71	0.32
186	409	84	1727	12.84	0.4	-0.24

Table 6.3: Table 6.2 continued

star	Webda	filter	No #	freq. F1[c/d]	amp. A1 [mag]	phase	noise [mag]	S/N
1	313	V	1	3.768	0.003	0.067	0.0016	1.801
2	299	V	1	3.737	0.002	0.357		
3	289	V	1	2.992	0.003	0.937	0.002	1.406
4	285	V	1	3.030	0.008	0.472	0.002	2.321
5	276	V	1	3.087	0.002	0.082	0.001	1.321
6	262	V	1	3.707	0.006	0.894	0.003	2.099
7	260	V	1	25.148	0.003	0.575	0.0002	10.132
8	240	V	1	4.060	0.001	0.296	0.001	2.236
9	237	V	1	4.011	0.004	0.331	0.002	2.088
10	232	V	1	3.882	0.002	0.367	0.001	1.594
11	218	V	1	4.015	0.105	0.884	0.043	2.438
12	211	V	1	3.011	0.004	0.913	0.002	2.091
13	149	V	1	2.992	0.004	0.499	0.002	2.454
14	162	V	1	3.490	0.005	0.706	0.002	2.169
15	203	V	1	4.110	0.003	0.634	0.002	1.617
16	200	V	1	4.053	0.003	0.074	0.001	1.899
17	233	V	1	4.026	0.003	0.738	0.001	2.276
18	238	V	1	3.045	0.003	0.437	0.002	1.600
19	174	V	1	3.015	0.004	0.534	0.002	2.031
20	194	V	1	3.057	0.002	0.297	0.002	1.455
21	265	V	1	4.015	0.015	0.363	0.007	2.261
22	282	V	1	15.161	0.003	0.427	0.001	2.507
23	291	V	1	4.026	0.004	0.776	0.002	1.841
24	325	V	1	3.026	0.003	0.859	0.002	2.269
25	337	V	1	3.003	0.002	0.747	0.001	2.054
26	283	V	1	4.049	0.003	0.427	0.001	1.901
27	278	V	1	45.389	0.002	0.516	0.001	2.274
28	263	V	1	4.045	0.004	0.806	0.002	2.358
29	193	V	1	4.053	0.005	0.084	0.002	2.698
30	169	V	1	4.053	0.001	0.067	0.001	2.001
31	167	V	1	3.946	0.002	0.157	0.001	1.962
32	142	V	1	3.015	0.003	0.570	0.002	1.995
33	134	V	1	19.507	0.004	0.613	0.003	1.223
34	415	V	1	4.045	0.005	0.826	0.002	2.260
35	416	V	1	3.022	0.005	0.247	0.002	2.222
36	419	V	1	3.027	0.005	0.674	0.002	2.125
37	369	V	1	3.460	0.029	0.895	0.012	2.343
38	361	V	1	3.003	0.011	0.206	0.004	2.912
39	359	V	1	3.011	0.011	0.468	0.006	1.899
40	355	V	1	4.399	0.001	0.550	0.001	1.933
41	375	V	1	4.049	0.003	0.464	0.002	2.014
42	388	V	1	3.741	0.002	0.791	0.001	1.827
43	396	V	1	4.018	0.005	0.593	0.003	1.596
44	427	V	1	5.071	0.005	0.072	0.002	1.925
45	395	V	1	6.486	0.002	0.719	0.001	2.498
46	366	V	1	3.011	0.002	0.930	0.001	2.751
47	360	V	1	3.737	0.002	0.918	0.002	1.576
48	336	V	1	3.068	0.002	0.075	0.001	1.797
49	349	V	1	4.015	0.035	0.395	0.014	2.457
50	323	V	1	3.003	0.003	0.733	0.002	1.743
51	273	V	1	3.999	0.002	0.600	0.001	1.662
52	252	V	1	3.342	0.001	0.612	0.001	1.702
53	227	V	1	3.376	0.052	0.130	0.045	1.156
54	199	V	1	4.775	0.003	0.227	0.002	1.648
55	171	V	1	3.988	0.003	0.224	0.002	1.592

Table 6.4: Frequencies of highest amplitudes for all stars in NGC 6611 in the V filter.

star	Webda	filter	No #	freq. F1[c/d]	amp. A1 [mag]	phase	noise [mag]	S/N
56	164	V	1	4.060	0.003	0.305	0.002	1.910
57	159	V	1	26.407	0.004	0.967	0.003	1.317
58	143	V	1	4.007	0.005	0.343	0.003	1.748
59	140	V	1	95.229	0.002	0.960	0.001	1.350
60	153	V	1	56.839	0.005	0.391	0.004	1.133
61	231	V	1	3.011	0.003	0.944	0.002	1.773
62	251	V	1	3.011	0.004	0.956	0.002	1.830
63	266	V	1	90.268	0.002	0.902	0.002	1.369
64	267	V	1	3.581	0.003	0.843	0.002	2.005
65	322	V	1	3.722	0.004	0.889	0.002	1.804
66	297	V	1	3.923	0.002	0.016	0.001	1.611
67	306	V	1	3.007	0.002	0.301	0.001	1.955
68	305	V	1	3.003	0.005	0.715	0.002	2.683
69	186	V	1	4.467	0.004	0.029	0.002	1.752
70	259	V	1	4.003	0.043	0.591	0.019	2.275
71	221	V	1	9.316	0.010	0.171	0.0003	32.08
72	213	V	1	3.011	0.005	0.897	0.002	3.037
73	202	V	1	4.060	0.003	0.753	0.002	1.827
74	228	V	1	3.007	0.005	0.342	0.002	2.110
75	247	V	1	4.056	0.005	0.646	0.003	1.929
76	222	V	1	3.007	0.004	0.318	0.002	2.070
77	365	V	1	5.106	0.010	0.497	0.006	1.590
78	392	V	1	4.041	0.002	0.590	0.001	2.584
79	417	V	1	4.011	0.006	0.782	0.002	2.674
80	340	V	1	3.015	0.002	0.531	0.001	1.842
81	304	V	1	4.018	0.006	0.605	0.003	1.853
82	292	V	1	29.876	0.002	0.368	0.0002	7.947
83	261	V	1	4.083	0.010	0.853	0.006	1.650
84	151	V	1	3.456	0.002	0.203	0.001	1.915
85	117	V	1	4.003	0.020	0.575	0.009	2.316
86	118	V	1	3.019	0.005	0.622	0.002	2.409
87	121	V	1	4.003	0.011	0.095	0.005	2.346
88	110	V	1	3.011	0.008	0.393	0.003	2.382
89	161	V	1	3.999	0.053	0.007	0.023	2.335
90	144	V	1	3.019	0.005	0.585	0.001	4.040
91	137	V	1	3.007	0.005	0.360	0.002	2.689
92	128	V	1	16.416	0.003	0.433	0.002	1.352
93	127	V	1	97.157	0.004	0.532	0.003	1.362
94	138	V	1	77.255	0.002	0.085	0.002	1.275
95	160	V	1	88.496	0.005	0.639	0.004	1.171
96	111	V	1	97.400	0.006	0.316	0.005	1.167
97	79	V	1	4.098	0.003	0.846	0.002	1.821
98	81	V	1	4.041	0.010	0.189	0.004	2.632
99	80	V	1	5.026	0.002	0.246	0.001	1.902
100	1887	V	1	3.007	0.010	0.814	0.004	2.836
101	49	V	1	2.996	0.017	0.448	0.004	4.278
102	56	V	1	3.007	0.008	0.794	0.003	2.991
103	67	V	1	4.041	0.006	0.196	0.002	2.488
104	59	V	1	3.011	0.009	0.425	0.003	2.600
105	48	V	1	3.011	0.009	0.395	0.003	3.678
106	73	V	1	3.003	0.007	0.186	0.002	3.738
107	36	V	1	9.995	0.001	0.699	0.001	2.059
108	26	V	1	3.003	0.006	0.163	0.001	4.471
109	24	V	1	3.787	0.002	0.269	0.001	2.143
110	19	V	1	2.996	0.011	0.931	0.003	3.401

Table 6.5: Table 6.4 continued

star	Webda	filter	No #	freq. F1[c/d]	amp. A1 [mag]	phase	noise [mag]	S/N
111	17	V	1	3.965	0.006	0.096	0.003	2.119
112	90	V	1	4.015	0.031	0.394	0.013	2.339
113	96	V	1	3.049	0.004	0.528	0.002	2.233
114	101	V	1	81.839	0.003	0.890	0.002	1.268
115	89	V	1	4.056	0.005	0.642	0.002	2.191
116	82	V	1	89.047	0.002	0.885	0.002	1.509
117	132	V	1	78.467	0.007	0.468	0.005	1.262
118	148	V	1	98.628	0.002	0.902	0.002	1.354
119	41	V	1	4.087	0.002	0.057	0.001	1.568
120	25	V	1	6.033	0.002	0.429	0.001	2.216
121	-	V	1	4.003	0.007	0.134	0.003	2.093
122	52	V	1	4.007	0.006	0.754	0.003	1.873
123	1890	V	1	3.011	0.018	0.400	0.005	3.205
124	42	V	1	98.213	0.006	0.488	0.005	1.206
125	76	V	1	11.987	0.002	0.624	0.002	1.367
126	85	V	1	66.849	0.007	0.451	0.006	1.160
127	105	V	1	4.064	0.004	0.903	0.002	1.989
128	104	V	1	14.507	0.006	0.546	0.004	1.475
129	-	V	1	3.973	0.016	0.317	0.007	2.308
130	-	V	1	4.110	0.011	0.132	0.005	2.280
131	99	V	1	34.885	0.004	0.392	0.003	1.266
132	53	V	1	7.056	0.003	0.880	0.002	1.394
133	545	V	1	2.996	0.006	0.054	0.003	2.360
134	-	V	1	3.980	0.011	0.531	0.006	1.895
135	38	V	1	3.726	0.003	0.072	0.001	2.164
136	44	V	1	3.992	0.009	0.313	0.006	1.495
137	30	V	1	3.000	0.006	0.598	0.002	2.465
138	33	V	1	3.034	0.005	0.057	0.002	2.750
139	21	V	1	4.015	0.005	0.937	0.002	2.221
140	-	V	1	3.969	0.011	0.710	0.006	2.021
141	61	V	1	27.163	0.004	0.598	0.003	1.457
142	106	V	1	23.567	0.004	0.889	0.003	1.325
143	136	V	1	4.049	0.005	0.390	0.003	1.886
144	91	V	1	3.992	0.010	0.361	0.005	1.933
145	1891	V	1	63.089	0.009	0.132	0.007	1.210
146	70	V	1	65.781	0.003	0.559	0.002	1.406
147	47	V	1	4.026	0.013	0.284	0.007	1.837
148	43	V	1	3.319	0.003	0.283	0.001	2.412
149	40	V	1	4.957	0.007	0.799	0.004	1.782
150	37	V	1	99.510	0.008	0.447	0.007	1.248
151	31	V	1	4.132	0.002	0.316	0.001	1.861
152	20	V	1	5.216	0.004	0.987	0.002	1.909
153	18	V	1	4.015	0.003	0.862	0.001	3.560
154	66	V	1	4.056	0.002	0.151	0.001	1.840
155	72	V	1	3.003	0.006	0.233	0.002	2.553
156	95	V	1	3.007	0.004	0.322	0.002	2.155
157	103	V	1	3.098	0.004	0.960	0.002	1.749
158	113	V	1	63.808	0.003	0.887	0.003	1.250
159	133	V	1	40.462	0.005	0.237	0.004	1.245
160	-	V	1	3.007	0.029	0.273	0.006	4.467
161	93	V	1	3.007	0.062	0.775	0.014	4.337
162	77	V	1	3.011	0.003	0.955	0.002	1.567
163	100	V	1	48.647	0.004	0.098	0.002	1.472
164	123	V	1	7.026	0.005	0.401	0.004	1.244
165	122	V	1	4.015	0.002	0.967	0.001	2.316

Table 6.6: Table 6.4 continued. For the stars marked with - there are no cross references with WEBDA.

star	Webda	filter	No #	freq. F1[c/d]	amp. A1 [mag]	phase	noise [mag]	S/N
166	112	V	1	3.003	0.002	0.728	0.001	1.719
167	35	V	1	4.554	0.003	0.175	0.001	2.245
168	39	V	1	3.049	0.004	0.543	0.002	1.940
169	625	V	1	19.104	0.001	0.337	0.001	1.883
170	50	V	1	3.015	0.005	0.035	0.002	2.819
171	64	V	1	4.037	0.003	0.141	0.001	1.740
172	74	V	1	4.015	0.003	0.968	0.002	1.895
173	188	V	1	4.475	0.006	0.792	0.005	1.303
174	255	V	1	3.003	0.005	0.683	0.001	3.056
175	256	V	1	3.003	0.005	0.708	0.002	2.966
176	269	V	1	4.045	0.002	0.305	0.001	1.967
177	406	V	1	4.007	0.021	0.177	0.009	2.461
178	402	V	1	4.003	0.034	0.596	0.015	2.298
179	400	V	1	3.338	0.002	0.920	0.001	1.613
180	374	V	1	7.739	0.011	0.192	0.0004	25.559
181	371	V	1	3.003	0.003	0.735	0.002	1.637
182	433	V	1	4.011	0.005	0.445	0.003	1.763
183	372	V	1	4.102	0.010	0.980	0.004	2.170
184	327	V	1	3.007	0.003	0.342	0.002	1.797
185	345	V	1	3.581	0.003	0.791	0.002	2.141
186	409	V	1	4.098	0.001	0.032	0.001	2.215

Table 6.7: Table 6.4 continued

star	Webda	filter	No #	freq. F1[c/d]	amp. A1 [mag]	phase	noise [mag]	S/N
1	313	B	1	3.007	0.004	0.079	0.002	2.100
2	299	B	1	4.091	0.003	0.689	0.001	2.179
3	289	B	1	4.099	0.004	0.971	0.002	2.070
4	285	B	1	3.007	0.005	0.154	0.002	2.633
5	276	B	1	4.406	0.002	0.761	0.001	1.956
6	262	B	1	4.121	0.007	0.624	0.003	2.167
7	260	B	1	25.151	0.003	0.047	0.0004	8.173
8	240	B	1	4.022	0.004	0.230	0.001	3.029
9	237	B	1	4.007	0.004	0.842	0.002	2.258
10	232	B	1	3.988	0.002	0.236	0.001	2.071
11	218	B	1	4.003	0.327	0.273	0.154	2.124
12	211	B	1	3.049	0.005	0.263	0.002	2.086
13	149	B	1	3.973	0.008	0.433	0.003	2.290
14	162	B	1	4.490	0.006	0.603	0.003	2.301
15	203	B	1	4.083	0.003	0.494	0.002	1.793
16	200	B	1	24.340	0.005	0.623	0.002	1.895
17	233	B	1	4.338	0.005	0.099	0.002	2.135
18	238	B	1	4.418	0.004	0.604	0.002	1.867
19	174	B	1	3.004	0.005	0.047	0.002	2.515
20	194	B	1	3.403	0.003	0.515	0.002	1.966
21	265	B	1	4.102	0.005	0.581	0.003	1.756
22	282	B	1	4.007	0.004	0.835	0.002	1.849
23	291	B	1	4.125	0.006	0.667	0.003	2.082
24	325	B	1	3.007	0.006	0.134	0.002	2.912
25	337	B	1	8.634	0.002	0.384	0.001	2.151
26	283	B	1	4.034	0.003	0.120	0.002	1.929
27	278	B	1	58.261	0.006	0.209	0.002	2.261
28	263	B	1	3.011	0.011	0.790	0.005	2.382
29	193	B	1	4.045	0.011	0.916	0.006	1.966
30	169	B	1	4.471	0.002	0.475	0.001	2.205

Table 6.8: Frequencies of highest amplitudes for all stars in NGC 6611 in the B filter.

star	Webda	filter	No #	freq. F1[c/d]	amp. A1 [mag]	phase	noise [mag]	S/N
31	167	B	1	94.970	0.004	0.387	0.002	1.928
32	142	B	1	3.004	0.008	0.997	0.002	3.893
33	134	B	1	19.436	0.009	0.886	0.008	1.182
34	415	B	1	4.129	0.005	0.248	0.002	2.101
35	416	B	1	4.030	0.007	0.446	0.002	2.989
36	419	B	1	4.053	0.006	0.138	0.003	2.271
37	369	B	1	5.456	0.103	0.932	0.066	1.554
38	361	B	1	3.011	0.018	0.769	0.008	2.389
39	359	B	1	4.076	0.012	0.839	0.007	1.768
40	355	B	1	3.004	0.004	0.506	0.001	3.256
41	375	B	1	4.471	0.004	0.620	0.002	2.068
42	388	B	1	4.003	0.004	0.185	0.002	2.470
43	396	B	1	4.015	0.011	0.084	0.007	1.584
44	427	B	1	3.996	0.009	0.463	0.006	1.636
45	395	B	1	5.053	0.005	0.959	0.002	2.375
46	366	B	1	3.005	0.009	0.818	0.002	4.143
47	360	B	1	4.083	0.004	0.102	0.002	2.113
48	336	B	1	4.003	0.004	0.161	0.002	2.301
49	349	B	1	3.004	0.015	0.021	0.004	3.889
50	323	B	1	4.099	0.003	0.941	0.001	2.109
51	273	B	1	4.859	0.002	0.536	0.001	1.862
52	252	B	1	3.988	0.003	0.335	0.002	1.860
53	227	B	1	3.380	0.054	0.986	0.047	1.151
54	199	B	1	4.102	0.004	0.211	0.002	1.827
55	171	B	1	4.118	0.005	0.908	0.002	2.239
56	164	B	1	4.399	0.006	0.092	0.004	1.505
57	159	B	1	75.131	0.010	0.752	0.008	1.266
58	143	B	1	13.208	0.012	0.729	0.008	1.439
59	140	B	1	89.476	0.004	0.566	0.004	1.206
60	153	B	1	42.392	0.008	0.293	0.006	1.206
61	231	B	1	4.091	0.003	0.750	0.002	1.883
62	251	B	1	3.315	0.004	0.688	0.002	2.215
63	266	B	1	58.604	0.005	0.469	0.005	1.186
64	267	B	1	3.007	0.007	0.151	0.003	2.603
65	322	B	1	3.718	0.005	0.398	0.003	1.883
66	297	B	1	4.003	0.004	0.195	0.002	2.396
67	306	B	1	4.102	0.002	0.614	0.001	1.792
68	305	B	1	3.007	0.005	0.663	0.002	2.629
69	186	B	1	4.194	0.008	0.646	0.005	1.464
70	259	B	1	4.969	0.008	0.016	0.004	1.887
71	221	B	1	9.317	0.013	0.348	0.0004	28.358
72	213	B	1	3.015	0.010	0.794	0.002	4.661
73	202	B	1	99.847	0.004	0.925	0.003	1.171
74	228	B	1	4.110	0.005	0.755	0.002	2.351
75	247	B	1	69.340	0.012	0.400	0.010	1.152
76	222	B	1	3.057	0.003	0.568	0.002	1.864
77	365	B	1	58.357	0.025	0.744	0.023	1.084
78	392	B	1	2.996	0.004	0.843	0.002	2.912
79	417	B	1	3.004	0.019	0.012	0.005	4.173
80	340	B	1	3.061	0.003	0.167	0.001	2.008
81	304	B	1	62.508	0.006	0.578	0.005	1.204
82	292	B	1	28.870	0.003	0.324	0.0004	8.081
83	261	B	1	5.121	0.017	0.769	0.010	1.680
84	151	B	1	12.436	0.007	0.487	0.006	1.131
85	117	B	1	3.004	0.019	0.020	0.005	4.008
86	118	B	1	95.521	0.009	0.184	0.009	1.104

Table 6.9: Table 6.8 continued

star	Webda	filter	No #	freq. F1[c/d]	amp. A1 [mag]	phase	noise [mag]	S/N
87	121	B	1	4.072	0.025	0.181	0.015	1.702
88	110	B	1	3.007	0.008	0.139	0.003	2.874
89	161	B	1	4.099	0.006	0.955	0.003	1.814
90	144	B	1	78.488	0.002	0.663	0.001	1.659
91	137	B	1	3.000	0.0186	0.434	0.005	3.590
92	128	B	1	7.410	0.006	0.647	0.005	1.246
93	127	B	1	48.277	0.007	0.176	0.007	1.082
94	138	B	1	4.007	0.005	0.865	0.004	1.439
95	160	B	1	64.402	0.009	0.216	0.008	1.190
96	111	B	1	32.321	0.014	0.265	0.012	1.224
97	79	B	1	4.083	0.003	0.480	0.002	2.125
98	81	B	1	63.729	0.018	0.366	0.015	1.214
99	80	B	1	56.722	0.003	0.159	0.002	1.216
100	1887	B	1	3.996	0.009	0.031	0.005	1.971
101	49	B	1	3.992	0.022	0.876	0.008	2.633
102	56	B	1	28.245	0.011	0.720	0.010	1.097
103	67	B	1	13.364	0.006	0.646	0.004	1.361
104	59	B	1	4.007	0.007	0.8617	0.005	1.593
105	48	B	1	4.030	0.016	0.485	0.007	2.260
106	73	B	1	14.927	0.010	0.431	0.007	1.281
107	36	B	1	5.091	0.002	0.458	0.001	2.005
108	26	B	1	3.004	0.005	0.489	0.001	4.166
109	24	B	1	5.608	0.004	0.954	0.002	2.026
110	19	B	1	4.118	0.012	0.523	0.007	1.696
111	17	B	1	39.145	0.010	0.028	0.008	1.154
112	90	B	1	5.152	0.012	0.232	0.007	1.707
113	96	B	1	79.572	0.008	0.840	0.007	1.235
114	101	B	1	62.079	0.008	0.366	0.007	1.168
115	89	B	1	75.081	0.007	0.204	0.006	1.202
116	82	B	1	6.068	0.009	0.018	0.006	1.314
117	132	B	1	3.901	0.016	0.542	0.007	2.079
118	148	B	1	2.996	0.011	0.836	0.004	3.001
119	41	B	1	4.064	0.003	0.467	0.002	1.960
120	25	B	1	4.000	0.004	0.501	0.001	2.972
121	-	B	1	4.129	0.013	0.292	0.009	1.486
122	52	B	1	5.133	0.014	0.592	0.009	1.486
123	1890	B	1	3.996	0.026	0.072	0.017	1.543
124	42	B	1	96.825	0.015	0.654	0.013	1.211
125	76	B	1	99.045	0.013	0.904	0.011	1.183
126	85	B	1	4.950	0.015	0.026	0.011	1.387
127	105	B	1	57.113	0.013	0.062	0.012	1.116
128	104	B	1	7.612	0.008	0.242	0.005	1.520
129	-	B	1	3.950	0.031	0.776	0.019	1.655
130	-	B	1	4.414	0.027	0.422	0.013	2.126
131	99	B	1	57.490	0.021	0.469	0.017	1.190
132	53	B	1	58.007	0.006	0.514	0.005	1.219
133	545	B	1	3.996	0.011	0.983	0.006	1.694
134	-	B	1	5.000	0.027	0.348	0.017	1.597
135	38	B	1	3.007	0.004	0.172	0.001	2.657
136	44	B	1	83.514	0.016	0.035	0.014	1.190
137	30	B	1	4.000	0.006	0.612	0.003	2.099
138	33	B	1	3.007	0.005	0.191	0.002	2.556
139	21	B	1	98.262	0.006	0.797	0.004	1.333
140	-	B	1	61.185	0.029	0.900	0.024	1.188
141	6	B	1	50.848	0.010	0.216	0.008	1.286
142	106	B	1	94.673	0.014	0.718	0.012	1.134

Table 6.10: Table 6.8 continued. For the stars marked with - there are no cross references with WEBDA.

star	Webda	filter	No #	freq. F1[c/d]	amp. A1 [mag]	phase	noise [mag]	S/N
143	136	B	1	57.592	0.012	0.443	0.010	1.116
144	91	B	1	42.818	0.024	0.643	0.020	1.203
145	1891	B	1	36.389	0.024	0.448	0.020	1.221
146	70	B	1	99.315	0.006	0.745	0.005	1.254
147	47	B	1	4.022	0.017	0.774	0.007	2.416
148	43	B	1	31.994	0.002	0.385	0.002	1.463
149	40	B	1	5.083	0.019	0.677	0.011	1.764
150	37	B	1	4.080	0.015	0.433	0.008	1.872
151	31	B	1	4.095	0.003	0.368	0.001	2.214
152	20	B	1	15.082	0.007	0.549	0.005	1.330
153	18	B	1	9.999	0.003	0.119	0.001	1.852
154	66	B	1	4.072	0.003	0.671	0.001	1.993
155	72	B	1	72.736	0.010	0.392	0.008	1.152
156	95	B	1	3.007	0.014	0.592	0.003	4.346
157	103	B	1	4.095	0.005	0.341	0.003	1.913
158	113	B	1	61.573	0.007	0.131	0.006	1.216
159	133	B	1	4.163	0.012	0.718	0.006	1.940
160	-	B	1	4.026	0.033	0.311	0.010	3.468
161	93	B	1	3.007	0.037	0.096	0.010	3.557
162	77	B	1	2.992	0.005	0.264	0.002	2.482
163	100	B	1	29.967	0.008	0.518	0.006	1.371
164	123	B	1	18.531	0.012	0.342	0.010	1.230
165	122	B	1	4.502	0.003	0.310	0.002	1.567
166	112	B	1	5.091	0.003	0.419	0.001	2.027
167	35	B	1	4.308	0.004	0.343	0.002	2.055
168	39	B	1	20.086	0.004	0.872	0.003	1.405
169	625	B	1	26.397	0.003	0.386	0.002	1.800
170	50	B	1	4.015	0.006	0.049	0.002	2.665
171	64	B	1	4.080	0.003	0.890	0.002	1.989
172	74	B	1	5.482	0.005	0.047	0.003	2.015
173	188	B	1	5.654	0.006	0.056	0.004	1.508
174	255	B	1	3.007	0.021	0.608	0.005	4.479
175	256	B	1	3.004	0.004	0.041	0.002	2.390
176	269	B	1	4.099	0.003	0.929	0.001	2.527
177	406	B	1	3.004	0.022	0.017	0.005	4.174
178	402	B	1	3.004	0.017	0.028	0.004	3.902
179	400	B	1	4.091	0.002	0.769	0.001	1.867
180	374	B	1	7.736	0.015	0.046	0.0004	32.930
181	371	B	1	4.102	0.004	0.551	0.002	2.239
182	433	B	1	4.038	0.007	0.729	0.003	2.376
183	372	B	1	5.121	0.012	0.781	0.006	1.823
184	327	B	1	3.984	0.003	0.751	0.002	1.956
185	345	B	1	3.589	0.004	0.214	0.002	2.096
186	409	B	1	3.007	0.009	0.098	0.002	3.988

Table 6.11: Table 6.8 continued. For the stars marked with - there are no cross references with WEBDA.

Bibliography

Aerts C., Christensen-Dalsgaard J., Kurtz D.W., 2010, *Asteroseismology*, Springer Verlag

Balona L.A., 1994, *Effective temperature, bolometric correction and mass calibration for O-F stars*, MNRAS, 268, 119-127

Bastian U., Finkenzeller U., Jaschek C., Jaschek M., 1983, *The definition of T Tauri and Herbig Ae/Be stars*, A&A, 126, 438-439

Beals C.S., Blanchet G.H., 1938, *An absorption line at $\lambda 4430.6$ of possibly interstellar origin*, MNRAS,98,398B

Belikov A.N., Kharchenko N.V., Piskunov A.E., Schilbach E., 1999, *The extremely young open cluster NGC 6611: Compiled catalogue, absorption map and the HR diagram*, A&AS, 134, 525-536

Belikov A.N., Kharchenko N.V., Piskunov A.E., Schilbach E., 2000, *The extremely young open cluster NGC 6611, luminosity function and star formation history*, A&A, 358, 886-896

Boehm T., Catala C., 1995, *Rotation, winds and active phenomena in Herbig Ae/Be stars*, A &A, 301, 155-169

Blondel P.F.C., Tjin A Djie H.R.E., 2006, *Modeling of PMS Ae/Fe stars using UV spectra*, A&A, 456, 1045-1068

Boesono B., Thé P.S., Tjin a djie H.R.E., 1987, *A study of the nature of the Hα-emission stars LkHα112, 115, 118, and 119*, Ap&SS, 137, 167B

Bosch G. L., Morrell N.I., Niemelae V.S., 1999, *Stellar spectroscopy in NGC 6611: binary frequency and new spectral types of several early type stars*, Revista Mexicana de Astronomia y Astrofisica, 35, 85-96

Breger M., 1972, *Pre-main sequence stars. I. Light variability, shells and pulsation in NGC 2264*, ApJ, 171, 539B

Breger M., Stich J., Garrido R., et al., 1993, A&A, 271, 482

Carmona A., van den Ancker M.E., Audard M., Henning Th., Setiawan J., Rodmann J., 2010, *New Herbig Ae/Be stars confirmed via high-resolution optical spectroscopy*, A&A, 517, 67

Catala C., 1994, *The spectroscopic variablitiy of the Herbig Ae/Be stars*, ASP Conference Series, Vol. 62

Catala C., Boehm T., Donati J.F., Simon T., Jiang S., Zhao F., 1997, *Short term variability of photospheric lines in the pre-main sequence Herbig Ae star AB Aurigae*, A&A, 319, 176-183

Chen L., de Grijs R., Zhao J.L., 2007, AJ, 134, 1368

Chini R., Neckel Th., 1981, *UBV and Hβ Observations of Stars towards M8*, A&A, 102, 171-174

Chini R., Wargau W.F., 1990, *Abnormal extinction and pre-main sequence stars in M16 (NGC 6611)*, A&A, 227, 213-219

Code A.D., 1958, *A pre-discovery observation of the diffuse interstellar band λ 4430*, PASP, 70, 407

di Criscienzo M.Di., Ventura P., Antona F., 2008, *Updated pre-main sequence tracks at low metallicities for 0.1* $\leq M/M_\odot \leq$ *1.5*, A&A, 496, 223D

di Criscienzo M., Ventura P., Antona F.D., Marconi M., Ruoppo A., 2008, *Matching the frequency spectrum of pre-main sequence stars by means of standard and rotating models*, MNRAS., 389, 325-332

de Winter D., Koulis C., Thé P.S., van den Ancker M.E., Pérez M.R. and Bibo E.A., 1997, *Pre-main sequence candidates in the very young open cluster NGC 6611*, A&AS, 121, 223-242

de Winter D., Thé P.S., 1991, *Candiates of pre-main sequence objects in the very young open cluster NGC 6611*, Mem. S.A.It., 62, 881D

Dufton P.L., Smartt S.J., Lee J.K., Ryans R.S.I., Hunter I., Evans C.J., Herrero A., Trundle C., Lennon D.J., Irwin M.J., Kaufer A., 2006, *The VLT-Flames survey of massive stars: stellar parameters and rotational velocities in NGC 3293, NGC 4755 and NGC 6611*, A&A, 457, 265-280

Eggen O.J., 1961, *Three colour photometry in the southern hemisphere: NGC 6383, NGC 6405 and standard stars*, R. Obs. Bull. No. 27

FitzGerald M.P., Jackson P.D., Luiken M., 1978, *NGC 6383 - I. The central core*, MNRAS, 182, 607-616

Frémat Y., Neiner C., Hubert A.-M., Floquet M., Zorec J., Janot-Pacheco E., Renan de Medeiros J., 2006, *Fundamental parameters of Be stars located in the seismology fields of COROT*, A&A, 451, 1053-1063

Gelbmann M., Kupka F., Weiss W.W., Mathys G., 1997, A&A, 319, 630 (Paper II)

Goetz W., 1972, *Untersuchungen ber die Struktur junger Sternhaufen und die Entwicklungsphasen ihrer Mitglieder III. NGC 6611*, Astron. Nachr., 294, 1-2

Gray D.F., 1992, *The observation and analysis of stellar photospheres*, Cambridge Astrophysics Series

Guarcello M.G., Micela G., Damiani F., Peres G., Prisinzano L., Sciortino S., 2009, *Correlation between the spatial distribution of circumstellar disks and massive stars in the young open cluster NGC 6611, II. Cluster members selected with Spitzer/IRAC*, A&A, 496, 453-463

Guarcello M.G., Prisinzano L., Micela G., Damiani F., Peres G., Sciortino S., 2007, *Correlation between the spatial distribution of circumstellar disks and massive stars in the open cluster NGC 6611*, A&A, 462, 245-255

Guenther D.B., Kallinger T., Zwintz K., Weiss W.W., Tanner J., 2007, *Seismology of pre-main sequence stars in NGC 6530*, ApJ, 671, 581-591

Guzik J.A., Kaye A.B., Bradley P.A., Cox A.N., Neuforge C., 2000, *Driving the gravity-mode pulsations in γ Doradus variables*, ApJ 542, 57

Gvaramadze V.V., Bomans D.J., 2008, *Search for OB stars running away from young stars clusters I. NGC 6611*, A&A, 490, 1071-1077

Herbig G. H., Dahm S. E., 2001, *On the Be and Ae Stars in NGC 6611*, PASP, 113, 195-196

Herbig G.H., 1959, *The spectra of Be- and Ae-type stars associated with nebulosity*, ApJS, 4, 337H

Herbig G.H., 1963, *The diffuse interstellar bands. I. A possible identification of λ 4430*, ApJ, 137, 200H

Herbig G.H., 1966, *The diffuse interstellar bands. II. The profile of λ4430 in HD 183143*, Zeitschrift fuer Astrophysik, 64, 512-517

Herbig G.H., 1975, *The diffuse interstellar bands. IV. The region 4400-6850 Å*, ApJ, 196, 129-160

Herbig G.H., Dahm S.E., 2001, *On the Be and Ae Stars in NGC 6611*, PASP, 113, 195-196

Hernandez J., Calvet N., Briceno C., Hartmann L., Berlind P., 2004, *Spectral analysis and classification of Herbig Ae/Be stars*, AJ, 127, 1682-1701

Hillenbrand L. A., Massey P., Strom S. E., Merrill K. M., 1993, *NGC 6611: A cluster caught in the act*, AJ, Vol. 106, 5

Hiltner W.A., Morgan W.W., Neff J.S., 1965, *Studies in spectral classification, II. The HR diagram of NGC 6530* ApJ, 141, 183 H

Jenniskens P., Désert F.-X., 1994, *A survey of diffuse interstellar bands (3800-8680 Å)*, A&AS, 106, 39-78

Johnson H.L., 1962, *The law of interstellar extinction*, B.A.N., 17, 2, 115-126

Kaiser A., 2006, *Determination of Fundamental Parameters with Strœmgren Photometry*, Astrophysics of Variable Stars, ASP Conference Series, Vol. 349

Kaler J.B., 1994, *Sterne und ihre Spektren*, Spektrum Akademischer Verlag

Kallinger T., 2005, *PODEX - PhOtometric Data Extractor*, CoAst, 146

Kallinger T., Reegen P., Weiss W. W., 2007, *A heuristic derivation of the uncertainty for frequency determination in time series data*, A&A, 481, 571-574

Kenyon S.J., Hartmann L., 1995, ApJS, 101, 117

Kharchenko N.V., Schilbach E., 1995, Astron. Nachr., 316, 91

Kharchenko N.V., Piskunov A.E., Roeser S., Schilbach E., Scholz R.-D., 2005, A&A, 438, 1163

Kumar B., Sagar R., Sanwal B. B. and Bessell M.S., 2004, *On the highly reddened members in six young galactic star clusters - a multiwavelength study*, MNRAS, 353, 3, 991-1014

Kupka F., Piskunov N., Ryabchikova T.A., Stempels H.C., Weiss W.W., 1999, *VALD-2: Progress of the Vienna Atomic Line Data Base*, A&AS, 138, 119-133

Kurucz R. L., 2005, *Physical, numerical, and computational limits for Kurucz codes*, Mem. S. A. It. Suppl. Vol. 8, 73

Kurtz D.W., Marang, F., 1995, MNRAS, 276, 191K

Kuschnig R., Weiss W.W., Gruber R., Bely P.Y., Jenkner H., 1997, A&A, 328, 544

Lenz P., Breger M., 2005, *Period04 User Guide*, CoAst, 146, 53

Lloyd T. E., 1978, *The open cluster NGC 6383*, MNRAS, 184, 661-676

Marconi M., Palla F., 2004, *Pre-main sequence A-type stars*, The A star puzzle, Proceedings IAU Symposium, 224

Martayan C., Floquet M., Frémat Y., Hubert A.-M., Neiner C., Baade D., Fabregat J., 2009, *Early-type PMS and MS objects in M16 and the Carina star-forming regions*, Highlights of Astronomy, Vol. 14

Martayan C., Floquet M., Hubert A.-M., Fabregat J., Frémat Y., Baade D., Neiner C., 2007, *On the nature of early-type emission line objects in NGC 6611*, Société Francaise dAstronomie et dAstrophysique

Martayan C., Floquet M., Hubert A.M., Neiner C., Frémat Y., Baade D., Fabregat J., 2008, *Early type objects in NGC 6611 and Eagle Nebula*, A&A, 489, 456

Martin E.L., 1997, *Quantitative spectroscopic criteria for the classification of pre-main sequence low-mass stars*, A&A, 312, 492-496

Massey P., 1997, *A users guide to CCD reductions with IRAF*

Nesvacil N., Stuetz C., Weiss W. W., 2003, *ATLAS model atmospheres*, GAIA Spectroscopy, Science and Technology, ASP Conference Series, Vol. 298

Palla F., Stahler S.W., 2002, *Star Formation on space and time: Taurus-Auriga*, ApJ, 581, 1194-1203

Paunzen E., Zwintz K., Maitzen H.M., Pintado O.I., Rode-Paunzen M., 2004, *New variable stars in open clusters, I. Methods and results for 20 open clusters*, A&A, 418, 99-102

Piskunov N., Kupka F., 2001, *Model atmospheres with individualized abundances*, ApJ, 547, 1040-1056

Piskunov N., Kupka F., Ryabchikova T. A., Weiss W. W., Jeffery C.S., 1995, *VALD: The Vienna Atomic Line Database*, A&AS, 112, 525-535

Piskunov N., 1998, Cont. Astron. Obs. Skalnate Pleso, 27, 376

Rauw G., Becker M., Gosset E., Pittard J.M., Stevens I.R., 2003, *An XMM-Newton observation of the very young open cluster NGC 6383*, A&A, 407, 925-934

Rauw G., Manfroid J., de Becker M., 2010, *A photometric and spectroscopic investigation of star formation in the very young open cluster NGC 6383*, A&A, 511, A25

Reegen P., 2004, *SigSpec - Reliable Computation of Significance in Fourier Space*, The A-Star Puzzle, Proceedings IAU Symposium, 224

Reegen P., 2007, *Sig Spec - 1. Frequency- and phase-resolved significance in Fourier space*, A&A, 467, 1353-1371

Reegen P., 2007, *SigSpec 2.0 Users Manual*, CoAst

Reipurth B., Pedrosa A., Lago M.T.V.T., 1996, *Hα emission in pre-main sequence stars. I. An atlas of line profiles*, A&AS, 120, 229-256

Ripepi V., Marconi M,, Palla F., Bernabei S., 2006, *δ Scuti pulsation among pre-main sequence intermediate-mass stars*, Mem. S.A. It. Suppl., Vol. 9, 200

Sagar R., Joshi U.C., 1979, *A study of the young cluster NGC 6611*, Ap&SS, 66, 3S

Schmidt-Kaler, 1965, in Landolt-Boernstein, *Numerical data and functional relationships in science and technology*, group IV, Vol I, 284, Springer Verlag, Berlin

Sharpless S., 1953, *A catalogue of emission nebulae near the galactic plane*, ApJ, 118, 362

Shelyag S., Schuessler M., Solanki S.K., Berdyugina S.V., Voegler A., 2004, A&A, 427, 335-343

Stahler S., Palla F., 2006, *The formation of stars*, WILEY-VCH

Stahler S., 1983, ApJ, 274, 822

Sung H., Chun M., Bessel M., 2000, AJ, 120, 333

Talavera A., 1998, *Herbig Ae/Be stars: mass flows and disks*, ESA-SP, 413, 69T

Thé P.S., de Winter D., Feinstein A., Westerlund B.E., 1990, *The extinction law, the distance and the HR diagram of the extremely young open cluster NGC 6611*, A&AS, 82, 319-330

Thé P.S., Hageman T., Westerlund B.E., Tjin a Djie H.R.E., 1985, *The spectral energy distribution of stars above the ZAMS in the central part of the open cluster NGC 6383*, A&A, 151, 391-398

Tuchole H.-J., Geffert M., Thé P.S., 1986, *The proper motion and membership of stars in the very young open cluster NGC 6611*, A&AS, 66, 311-322

Valenti J.A., Piskunov N., 1996, *Spectroscopy made easy: A new tool for fitting observations with synthetic spectra*, A&AS, 118, 595-603

van Altena W.F., Jones B.F., 1972, *Membership in the extremely young open cluster NGC 6530 (M8)*, A&A, 20, 425-436

van den Ancker M.E., Thé P.S., de Winter D., 2000, *The central part of the young open cluster NGC 6383*, A&A, 362, 580-584

van den Ancker M.E., Thé P.S., Feinstein A., Vázquez R.A., de Winter D., Pérez M.R., 1997, *A multiwavelength study of star formation in the very young open cluster NGC 6530*, A&AS, 123, 63-82

Vieira S.L.A., Corradi W.J.B., Alencar S.H.P., Mendes L.T.S., Torres C.A.O., Quast G.R., Guimaraes M.M., Silva L., 2003, *Investigation of 131 Herbig Ae/Be candidate stars*, AJ, 126, 2971-2987

Walborn N.R., Fitzpatrick E.L., 1990, *Contemporary optical spectral classification of the OB stars: a digital atlas*, PASP, 102, 379-411

Walker M.F., 1957, *A study of extremely young clusters of stars*, ApJ, 63, 37

Walker M.F., 1957, *Studies of extremely young clusters II. NGC 6530*, ApJ., 125, 636

Walker M.F., 1961, *Studies of extremely young clusters. IV NGC 6611*, ApJ, 133, 438

Weigert A., Wendker H.J., Wisotzki L., 2005, *Astronomie und Astrophysik*, WILEY-VCH Verlag

Zug R.S., 1937, *Color excess in three open clusters in Sagittarius*, Lick Observatory Bulletin, 18, 892

Zwintz K., 2005, *Pulsating Pre-Main Sequence Stars in Young Open Clusters*, Dissertation, University of Vienna

Zwintz K., Marconi M., Reegen P., Weiss W.W., 2005, *Search for pulsating pre-main sequence stars in NGC 6383*, MNRAS, 357, 345-353

Zwintz K., Weiss W.W., 2006, *Pulsating pre-main sequence stars in IC 4996 and NGC 6530*, A&A, 457, 237-248

Danksagung

Zuerst möchte ich mich bei Konstanze Zwintz bedanken, die mir dieses spannende Thema ermöglicht hat und die mir in all der Zeit mit Rat und Tat zur Seite stand. Sie hatte immer ein offenes Ohr für mich und meinen Kummer und Sorgen und förderte mich in allen meinen Tätigkeiten. Desweiteren möchte ich mich bei Werner Weiss bedanken, der mir die Möglichkeit gab in seiner Arbeitsgruppe mitzuwirken, wodurch ich viel über Photometrie und Spektroskopie lernen durfte. Danken möchte ich auch Nicole Nesvacil, die die photometrischen Daten beobachtet hat und die bei spektroskopischen Belangen hilfreich zur Seite stand. Allen Dreien danke ich auch besonders für das Verständis, dass ich Beruf und Studium unter einen Hut bringen konnte.

Ich möchte mich auch bei Markus Hareter und Alexander Kaiser bedanken, die nicht nur bei Computerproblemen aushelfen konnten, sondern mit denen sich viele nette Gespräche im Laufe der Zeit ergeben haben und die stets aufmunternde Worte fanden. Ganz besonders danken möchte ich auch meinen Studienkollegen Ewald Grohs, Günter Ramberger und Michael Schulreich ausprechen, mit denen ich ein ganz besonderes Band der Freundschaft verbinde und denen ich eine besonders nette und tolle Studienzeit verdanke. Auch Piet Regen möchte ich danken, der stets auch ein offenes Ohr für mich gefunden hat.

Zum Abschluss möchte ich auch noch meinem Mann Wolfgang, meinem Bruder Alexander und meinen Eltern danken, die mich in all der Zeit sehr unterstützt und mir viel Geduld entgegengebracht haben.

Lebenslauf

Mag.[a] Susanne Pollack-Drs Bakk.

geboren in Wien, am 19. August 1973

1979-1983	Volksschule in Wien 5
1983-1992	neusprachliches Gymnasium in Wien 5
Juni 1992	Reifeprüfung
1992-1999	Lehramtsstudium Biologie und Erdwissenschaften
Mai 1999	Diplomprüfung
1997-2003	Ergänzungsstudium Lehramt Mathematik
2003-2007	Bakkalaureatsstudium Astronomie
März 2007	Abschluss des Bakkalaureatstudiums
seit 2007	Magisterstudium der Astronomie

Berufspraxis

SS 1996	Institut für Paläontologie
Sommer 1996	Akademie der Wissenschaften
WS 1996	Institut für Paläontologie
Sommer 1997	Institut für Paläontologie
1997-2005	Naturhistorisches Museum, Abteilung für Meteoritenkunde
1999-2000	Unterrichtspraktikum am GRG 14
seit 1999	HTL Spengergasse
2005-2009	KMS Kinkplatz Wien 14 - Kooperationslehrerin